Hybrid Pulse Position Modulation/Ultrashort Light Pulse Code-Division Multiple-Access Systems—Part I: Fundamental Analysis

Kwang Soon Kim, *Member, IEEE*, Dan M. Marom, *Member, IEEE*, Laurence B. Milstein, *Fellow, IEEE*, and Yeshaiahu Fainman, *Senior Member, IEEE*

***Abstract*—In this paper, we propose a hybrid pulse position modulation/ultrashort light pulse code-division multiple-access (PPM/ULP-CDMA) system for ultrafast optical communications. The proposed system employs spectral CDMA encoding/decoding and PPM with very short pulse separation. The statistical properties of the encoded ULP are investigated with a general pulse model, and the performance of the proposed PPM/ULP-CDMA system is investigated. It is shown that we can improve upon the performance of other ULP-CDMA systems, such as those using on–off keying, by employing PPM. It is also shown that we can improve the performance of the proposed system by increasing the effective number of chips, by increasing the number of PPM symbols, and by reducing the ULP duration. The performance analysis shows that the aggregate throughput of the proposed PPM/ULP-CDMA system could be over 1 Tb/s.**

***Index Terms*—optical code-division multiple-access (CDMA), pulse position modulation (PPM), ultrashort light pulse.**

I. Introduction

In recent years, design and analysis of optical communication networks has been an active research area, as it is commonly felt that a fiber-based optical communication network is the only way to meet the drastically increasing demand for multimedia services in the near future. Although wavelength-division multiplexing (WDM) is the current favorite multiplexing technology for optical communication [1], code-division multiple access (CDMA) can be a desirable alternative, since it would provide asynchronous access to a network, a degree of security against interception, no need for either frequency (or time) allocation or guard bands because of complete utilization of the time and frequency by each user, and simplified network control.

Additionally, techniques of high-resolution waveform synthesis by spectral filtering of ultrashort light pulses (ULPs) in an optical processor have been developed, advancing the science of ultrafast phenomena. By employing an orthogonal phase code set as the spectral filter, the resulting optical waveforms can be used as a basis for a multiuser communication system with a spread time property [2]. In the ULP-CDMA format suggested by Weiner, *et al.* [3], [4], each user has a unique phase code from the orthogonal set for encoding a pulse before transmission on a common optical fiber carrier in an on–off keying (OOK) modulation format. The desired signal is restored to a short pulse form (i.e., despread) at the receiver by applying a spectral filter consisting of the phase-conjugated code used at the transmitter of interest. The optical waveforms from other users remain as encoded pulses with long duration and low intensity. The decoded signal needs to be detected by a nonlinear thresholding operation [5], as the temporal variation of the signal is too fast for direct electronic detection schemes.

On the other hand, in many recent studies including [6]–[10], various kinds of pulse position modulation (PPM) have been investigated as ways to improve the performance of optical communication systems. In [11] and [12], however, it was shown that, for a fixed throughput and chip time, there is no advantage in employing conventional PPM in place of OOK in optical CDMA systems. Thus, some modified schemes, including overlapping PPM (OPPM) [11], [13] and bipolar PPM with spectral CDMA encoding [14], have been investigated to increase the bandwidth efficiency. In the ULP-CDMA systems, however, the situation is different. Since a large bandwidth (ultrashort pulsewidth) is already a given, it is of importance to determine how to utilize the bandwidth effectively. Recently, a ULP-CDMA system with PPM signaling has been reported in [15]. In this scheme, however, PPM is employed as it has been done in spread spectrum CDMA systems: the pulse separation of the PPM is greater than the encoded signal duration. Thus, the large bandwidth of the ULP is not fully exploited and the maximum number, M, of PPM symbols is given by the ratio of the symbol period to the CDMA encoded signal duration. One possible approach for better utilizing the large bandwidth of the ULP is to introduce PPM with a very small pulse separation symbol encoding. Then, the bandwidth efficiency would increase if we increase the number of PPM symbols roughly up to the ratio of the symbol period to the ULP duration. In

Paper approved by I. Andonovic, the Editor for Optical Networks and Devices of the IEEE Communications Society. Manuscript received May 17, 2001; revised March 25, 2002. This work was supported by National Science Foundation (NSF). The work of K. S. Kim and D. M. Marom was supported by the Korea Science and Engineering Foundation (KOSEF) and the Fannie and John Hertz Foundation, respectively.

K. S. Kim was with the Department of Electrical and Computer Engineering, University of California, San Diego, La Jolla, CA 92093 USA. He is now with the Mobile Telecommunication Research Laboratory, Electronics and Telecommunication Research Institute, Daejeon 305-350, Korea (e-mail: kwangsoon@etri.re.kr).

D. M. Marom was with the Department of Electrical and Computer Engineering, University of California, San Diego, La Jolla, CA 92093 USA. He is now with Advanced Photonics Research, Bell Laboratories, Lucent Technologies, Holmdel, NJ 07733 USA (e-mail: dmarom@lucent.com).

L. B. Milstein and Y. Fainman are with the Department of Electrical and Computer Engineering, University of California, San Diego, La Jolla, CA 92093-0407 (e-mail: milstein@ece.ucsd.edu; fainman@ece.ucsd.edu).

Digital Object Identifier 10.1109/TCOMM.2002.806501

this scheme, however, a detector with very high time resolution is necessary to discriminate the pulse positions. A new technique for converting ultrafast temporal information to a spatial image [16] may assist in the implementation of a high-resolution time filter at the receiver. The ability to observe the temporal signal by a spatial detector array enables parallel processing of received signals at all PPM signal locations. Thus, the proposed PPM scheme using the ULP with very short pulse separation can be implemented with electrical circuitry that is compatible with the symbol rate (typically, much lower than 1 GHz).

In this paper, we propose a hybrid PPM/ULP-CDMA scheme for ultrafast optical communications. The analysis of the proposed scheme spans two papers: Part I investigates the statistical properties of an ULP-CDMA network with a general pulse model, and provides a theoretical analysis on the performance of the proposed hybrid PPM/ULP-CDMA scheme; in Part II, we consider some issues on practical system implementation and their effects on the performance, as well as modified modulation/detection schemes to enhance the proposed PPM/ULP-CDMA system. The contributions of Part I of this paper include the following:

- the statistical properties of encoded ULPs are investigated based on a general pulse model;
- the performance of the proposed PPM/ULP-CDMA system is analyzed by assuming fully asynchronous transmission and taking the time-varying characteristics of the encoded ULP into account, which were not fully considered in [4] and [15].

II. Statistical Properties of Encoded ULPs

There is a need for re-evaluating the statistical properties of coded ULP because the previous analysis [4] only treated a simplified model where the spectrum had a rectangular shape. More representative pulse shapes of an actual ULP from mode-locked lasers are the Gaussian and sech profiles [17]. The structure of this section closely follows that in [4], including the statistical properties of a single-coded pulse and the correlation functions of the coded pulses. However, in this paper, we do not confine our consideration to a specific pulse shape.

We begin with a normalized and dimensionless (both in domain and in range) baseband temporal pulse shape $p_u(t)$ with the following properties: i) $p_u(t)$ is real; ii) the duration and the peak value of $p_u^2(t)$ are both one (for pulses not limited in the time domain, the duration is defined in the full-width half-maximum (FWHM) sense); iii) $|p_u(t)|$ is bounded by a function that is positive, monotonically decreasing with $|t|$, and integrable; iv) $\alpha_n \triangleq \int_{-\infty}^{\infty} p_u^n(t)\,dt > 0$, $n = 1, 2$. Note that α_n is also dimensionless because the domain and range of $p_u(t)$ are dimensionless. Also note that $P_u(\omega) \triangleq \int_{-\infty}^{\infty} p_u(t)\exp(-j\omega t)\,dt$ exists from property iii), where its FWHM bandwidth will be denoted as B. From the above properties, we get $\alpha_n < \alpha < \infty$ for $n = 1, 2$, where $\alpha \triangleq \int_{-\infty}^{\infty} |p_u(t)|\,dt$. Then, an input ULP with duration τ and its associated spectrum are given by

$$p(t) = \sqrt{P_0}\, p_u\left(\frac{t}{\tau}\right)\exp(j\omega_0 t)$$
$$\Leftrightarrow P(\omega) = \sqrt{P_0}\,\tau P_u(\tau(\omega - \omega_0)) \tag{1}$$

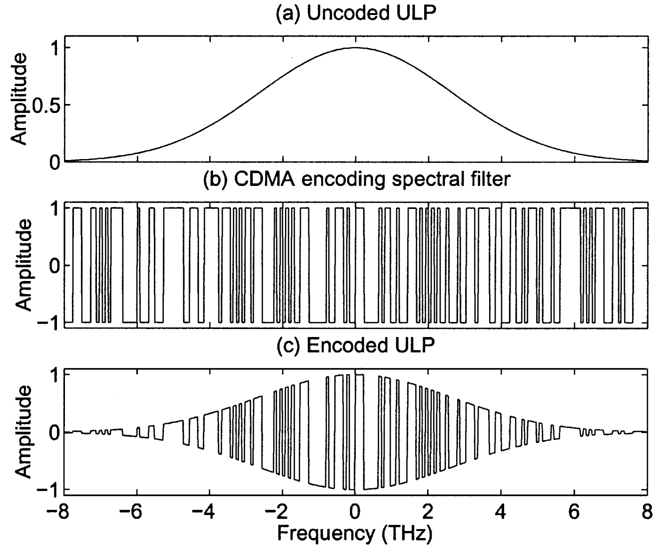

Fig. 1. Schematic of spectrally encoding an ULP. (a) Spectrum of Gaussian ULP. (b) Spectral binary encoding sequence. (c) Resultant spectrum of an encoded Gaussian ULP.

where P_0 is the peak power of the pulse, and ω_0 is the optical carrier frequency.

In the ULP-CDMA communication format, each user encodes his transmitted pulse with a unique spectral filter. The spectral filter is comprised of contiguous rectangular frequency bands, each of bandwidth Ω, where each band is multiplied by an element of a coding sequence. The encoding filter is realized by a spatial mask placed in the central Fourier plane of a spectral processing device—a standard optical setup consisting of a pair of gratings and lenses in a 4-f configuration—where the spectral components of the input ULP are spatially dispersed. The spectral filter can be implemented by either an etched mask or a spatial light modulator [18]. For the purpose of this analysis, we assume the elements of the code take on the values of ± 1 (i.e., a binary code) with equal probability. Note that the analysis can be generalized to a broader set of complex signature codes [19]. By using these quantized phase codes with alphabet size greater than two, the number of available signature sequences is greatly enlarged, thus supporting many users. Also, the optical implementation of the encoding filter using quantized phase codes is not significantly more difficult than implementing binary codes, as opposed to the radio frequency (RF) case where more hardware is required.

Since the bandwidth of the ULP may not be finite for certain pulse envelopes, we model the code as having an infinite number of elements. In practice, its truncated version is used, and one of the results of the following analysis is that we find the effective number of code elements contained in the bandwidth of the ULP, dependent on the pulse shape we assume.

A graphical representation of the encoding process is displayed in Fig. 1. The spectrum of an encoded pulse is given by

$$\begin{aligned} Y_i(\omega) &= P(\omega)H_i(\omega) \\ &= \sqrt{P_0}\,\tau P_u(\tau(\omega - \omega_0)) \sum_{m=-\infty}^{\infty} a_m^{(i)} g\left(\frac{\omega - \omega_0}{2\pi\Omega} - m\right) \end{aligned} \tag{2}$$

where $Y_i(\omega)$ is the spectrum of the encoded waveform of user i, $H_i(\omega)$ is the encoding filter of user i, $g(x) = 1$ when $|x| < 1/2$ and $g(x) = 0$, otherwise, Ω is the spectral chip bandwidth (in Hz), and $a_m^{(i)}$ is the mth element in the sequence used by user i. Then, the encoded output waveform is given by

$$\begin{aligned} y_i(t) &= \mathrm{FT}^{-1}\{Y_i(\omega)\} \\ &= \sqrt{P_0}\,\Omega\exp(j\omega_0 t) \\ &\quad\cdot\left[P_u\left(\frac{t}{\tau}\right)\otimes\left(\mathrm{sinc}(\Omega t)\sum_{m=-\infty}^{\infty}a_m^{(i)}\exp(j2\pi m\Omega t)\right)\right] \\ &= \sqrt{P_0\Omega}\,\exp(j\omega_0 t)\sum_{m=-\infty}^{\infty}a_m^{(i)}s_m(t) \end{aligned} \tag{3}$$

where $\mathrm{FT}^{-1}\{\cdot\}$ is the inverse Fourier transform, $\otimes$ is the convolution operator, $\mathrm{sinc}(x) \triangleq \sin(\pi x)/(\pi x)$, the second equality follows the fact that

$$\begin{aligned} &\mathrm{FT}^{-1}\left\{g\left(\frac{\omega-\omega_0}{2\pi\Omega}-m\right)\right\} \\ &\quad= \Omega\,\mathrm{sinc}(\Omega t)\cdot\exp(j\omega_0 t)\exp(j2\pi m\Omega t) \end{aligned}$$

and

$$s_m(t) \triangleq \sqrt{\Omega}\int_{-\infty}^{\infty}p_u\left(\frac{t-\sigma}{\tau}\right)\mathrm{sinc}(\Omega\sigma)\exp(j2\pi m\Omega\sigma)\,d\sigma.$$

Equation (3) describes the temporal evolution of an encoded waveform for a known encoding sequence. When $\Omega\tau \ll 1$, the envelope of the encoded waveform is determined by the $\mathrm{sinc}(\cdot)$ function, while the infinite sum results in a waveform that resembles a noise burst.

For the purpose of this analysis, we model the elements of the code, $a_m^{(i)}$, as uncorrelated binary random variables. In addition, we make the following definitions:

$$\begin{aligned} G_1(t, t_0) &\triangleq \sum_{m=-\infty}^{\infty}s_m(t)s_m^*(t+t_0) \\ &= \sum_{n=-\infty}^{\infty}\int_{-\infty}^{\infty}p_\tau(t-\sigma)p_\tau(t+t_0-\sigma-n/\Omega) \\ &\quad\cdot\mathrm{sinc}(\Omega\sigma)\,\mathrm{sinc}(\Omega\sigma+n)\,d\sigma \end{aligned} \tag{4}$$

$$\begin{aligned} G_2(t, t_0) &\triangleq \sum_{m=-\infty}^{\infty}s_m(t)s_m(t+t_0) \\ &= \sum_{n=-\infty}^{\infty}\int_{-\infty}^{\infty}p_\tau(t-\sigma)p_\tau(t+t_0+\sigma+n/\Omega) \\ &\quad\cdot\mathrm{sinc}(\Omega\sigma)\,\mathrm{sinc}(\Omega\sigma+n)\,d\sigma \end{aligned} \tag{5}$$

$$\begin{aligned} G_3(t, t_0) &\triangleq \sum_{m=-\infty}^{\infty}|s_m(t)|^2|s_m(t+t_0)|^2 \\ &= \Omega\sum_{n=-\infty}^{\infty}\int_{-\infty}^{\infty}\int_{-\infty}^{\infty}\int_{-\infty}^{\infty}p_\tau(t-\sigma_1)p_\tau(t-\sigma_2) \\ &\quad\cdot p_\tau(t+t_0-\sigma_3)p_\tau(t+t_0-\sigma_1+\sigma_2-\sigma_3-n/\Omega) \\ &\quad\cdot\mathrm{sinc}(\Omega\sigma_1)\,\mathrm{sinc}(\Omega\sigma_2)\,\mathrm{sinc}(\Omega\sigma_3) \\ &\quad\cdot\mathrm{sinc}(\Omega(\sigma_1-\sigma_2+\sigma_3)+n)\,d\sigma_1\,d\sigma_2\,d\sigma_3 \end{aligned} \tag{6}$$

where $p_\tau(t) = p_u(t/\tau)$, as well as

$$\begin{aligned} R_p(t_0) &\triangleq \frac{1}{\alpha_2}\int_{-\infty}^{\infty}p_u(t)p_u(t+t_0)\,dt, \\ p_2(t) &\triangleq \frac{1}{\alpha_2}\int_{-\infty}^{\infty}p_u(\sigma)p_u(t-\sigma)\,d\sigma \\ R_{\mathrm{sinc}}(t_0) &\triangleq \int_{-\infty}^{\infty}\mathrm{sinc}(t)\,\mathrm{sinc}(t+t_0)\,dt \end{aligned}$$

and

$$R_{\mathrm{sinc}^2}(t_0) \triangleq \int_{-\infty}^{\infty}\mathrm{sinc}^2(t)\,\mathrm{sinc}^2(t+t_0)\,dt.$$

In (4)–(6), the Fourier series identity $\Omega\sum_{m=-\infty}^{\infty}\exp(j2\pi m\Omega t) = \sum_{n=-\infty}^{\infty}\delta(t+n/\Omega)$ is used, where $\delta(\cdot)$ is the Dirac-delta function. With these definitions, statistical properties of an encoded waveform can now be inferred.

Proposition 1: The first and second moments of the encoded pulse $y_i(t)$ are $E\{y_i(t)\} = 0$ and $E\{y_i(t)y_i^*(t+t_0)\} = P_0\Omega\exp(-j\omega_0 t_0)G_1(t, t_0)$.

Proof: Since $E\{a_m^{(i)}\} = 0$, it is straightforward that $E\{y_i(t)\} = 0$ from (3). Again, from (3), we find the second moment of the encoded pulse as

$$\begin{aligned} &E\{y_i(t)y_i^*(t+t_0)\} \\ &\quad= P_0\Omega\exp(-j\omega_0 t_0)\sum_{m=-\infty}^{\infty}\sum_{n=-\infty}^{\infty}E\left\{a_m^{(i)}a_n^{(i)}\right\} \\ &\quad\cdot s_m(t)s_n^*(t+t_0) \\ &\quad= P_0\Omega\exp(-j\omega_0 t_0)\sum_{m=-\infty}^{\infty}s_m(t)s_m^*(t+t_0) \\ &\quad= P_0\Omega\exp(-j\omega_0 t_0)G_1(t, t_0) \end{aligned} \tag{7}$$

where the second equality follows from the uncorrelated property of the code elements. ■

Lemma 1: If $\Omega\tau \ll 1$, we have

$$\begin{aligned} G_1(t, t_0) &\cong \alpha_2\tau\mathrm{sinc}(\Omega t)\,\mathrm{sinc}(\Omega(t+t_0)) \\ &\quad\cdot\sum_{n=-\infty}^{\infty}R_p\left(\frac{t_0}{\tau}-\frac{n}{\Omega\tau}\right) \end{aligned}$$

and

$$\begin{aligned} G_2(t, t_0) &\cong \alpha_2\tau\,\mathrm{sinc}(\Omega t)\mathrm{sinc}(\Omega(t+t_0)) \\ &\quad\cdot\sum_{n=-\infty}^{\infty}p_2\left(\frac{2t+t_0}{\tau}+\frac{n}{\Omega\tau}\right). \end{aligned}$$

Proof: Since $\Omega\tau \ll 1$, $\mathrm{sinc}(\Omega t)$ has a much wider envelope than does $p_\tau(t)$. Thus, we have

$$\begin{aligned} G_1(t, t_0) &= \sum_{n=-\infty}^{\infty}\int_{-\infty}^{\infty}p_\tau(t-\sigma)p_\tau(t+t_0-\sigma-n/\Omega) \\ &\quad\cdot\mathrm{sinc}(\Omega\sigma)\,\mathrm{sinc}(\Omega\sigma+n)\,d\sigma \\ &\cong \mathrm{sinc}(\Omega t)\,\mathrm{sinc}(\Omega(t+t_0))\sum_{n=-\infty}^{\infty}\int_{-\infty}^{\infty}p_\tau(t-\sigma) \\ &\quad\cdot p_\tau(t+t_0-\sigma-n/\Omega)\,d\sigma \\ &= \alpha_2\tau\mathrm{sinc}(\Omega t)\,\mathrm{sinc}(\Omega(t+t_0)) \\ &\quad\cdot\sum_{n=-\infty}^{\infty}R_p\left(\frac{t_0}{\tau}-\frac{n}{\Omega\tau}\right). \end{aligned} \tag{8}$$

Similarly, we get

$$G_2(t,\,t_0) = \sum_{n=-\infty}^{\infty} \int_{-\infty}^{\infty} p_\tau(t-\sigma) p_\tau(t+t_0+\sigma+n/\Omega) \cdot \operatorname{sinc}(\Omega\sigma)\operatorname{sinc}(\Omega\sigma+n)\,d\sigma \cong \alpha_2\tau \operatorname{sinc}(\Omega t)\operatorname{sinc}(\Omega(t+t_0)) \cdot \sum_{n=-\infty}^{\infty} p_2\left(\frac{2t+t_0}{\tau}+\frac{n}{\Omega\tau}\right). \tag{9}$$

■

Corollary 1: If $\Omega\tau \ll 1$, the expected intensity profile of an encoded waveform can be approximated as $E\{I_i(t)\} \cong (P_0/N_{\text{eff}})\operatorname{sinc}^2(\Omega t)$, where $I_i(t) = |y_i(t)|^2$ and $N_{\text{eff}} \triangleq 1/(\alpha_2\Omega\tau)$ is the effective number of chips.

Proof: Since $\Omega\tau \ll 1$, we have $G_1(t,\,0) \cong \alpha_2\tau \operatorname{sinc}^2(\Omega t)\sum_{n=-\infty}^{\infty} R_p(n/\Omega\tau)$ from *Lemma 1*. Thus, from *Proposition 1*, we get

$$E\{I_i(t)\} \cong P_0\alpha_2\Omega\tau\operatorname{sinc}^2(\Omega t)\sum_{n=-\infty}^{\infty} R_p\left(\frac{n}{\Omega\tau}\right).$$

Since $R_p(t)$ is the autocorrelation function of $p_u(t)$, its duration is (approximately) twice that of $p_u(t)$, which yields $R_p(t) \cong 0$ for $|t| \gg 1$. Thus, since $\Omega\tau \ll 1$, $R_p(n/\Omega\tau)$, $n \neq 0$, can be ignored. Therefore, we get $E\{I_i(t)\} \cong (P_0/N_{\text{eff}})\operatorname{sinc}^2(\Omega t)$. ■

Note that the field autocorrelation shown in *Proposition 1* is not a stationary function of time, and that the peak power of the expected intensity of an encoded waveform has dropped by a factor of N_{eff}, compared to the input ULP peak power. From *Corollary 1*, the FWHM duration of the expected intensity of an encoded waveform is now inversely proportional to Ω, while its power spectrum remains the same, since a phase-only linear filter was used. Since the duration of an ULP is τ, the resulting time-bandwidth product of the encoded waveform has increased proportional to $1/(\Omega\tau)$, that is, proportional to N_{eff}. We conclude that the effective number of chips is analogous to the processing gain in conventional spread spectrum systems, and determines the amount of time spreading. Additionally, the energy in the encoded pulse is equal to the energy in the input pulse, as can be shown by integrating the intensities of the input and the encoded ULP over $t \in (-\infty,\,\infty)$.

As a last step, we analyze the intensity autocorrelation of an encoded waveform as follows:

Proposition 2: If $\Omega\tau \ll 1$, the intensity autocorrelation is given by

$$E\{I_i(t)I_i(t+t_0)\} = P_0^2\Omega^2\left(G_1(t,\,0)G_1(t+t_0,\,0) + G_1^2(t,\,t_0) + G_2^2(t,\,t_0) - 2G_3(t,\,t_0)\right).$$

Proof: See Appendix A. ■

From *Propositions 1* and *2*, we can see that the field and intensity autocorrelations are not stationary functions of time. Physical measurements of the autocorrelations perform time integration by the slow electronics that detect the optical signal. By performing time integration on the nonstationary results of *Propositions 1* and *2*, we get the time-integrated field and intensity autocorrelations as follows:

Lemma 2:

$$\Omega\int_{-\infty}^{\infty} G_1(t,\,t_0)\,dt = \alpha_2\tau\sum_{n=-\infty}^{\infty} R_{\text{sinc}}(n)\cdot R_p\left(\frac{t_0}{\tau}-\frac{n}{\Omega\tau}\right).$$

Proof: By substituting $\nu = t-\sigma$, we can rewrite (4) as

$$G_1(t,\,t_0) = \sum_{n=-\infty}^{\infty}\int_{-\infty}^{\infty} p_\tau(\nu)p_\tau(\nu+t_0-n/\Omega) \cdot\operatorname{sinc}(\Omega(t-\nu))\operatorname{sinc}(\Omega(t-\nu)+n)\,d\nu. \tag{10}$$

Thus, we have

$$\Omega\int_{-\infty}^{\infty} G_1(t,\,t_0)\,dt = \sum_{n=-\infty}^{\infty} R_{\text{sinc}}(n)\int_{-\infty}^{\infty} p_\tau(\nu)p_\tau(\nu+t_0-n/\Omega)\,d\nu = \alpha_2\tau\sum_{n=-\infty}^{\infty} R_{\text{sinc}}(n)\cdot R_p\left(\frac{t_0}{\tau}-\frac{n}{\Omega\tau}\right).$$

■

Proposition 3: The time-integrated field autocorrelation is given by

$$\Omega\int_{-\infty}^{\infty} y_i(t)y_i^*(t+t_0)\,dt = \frac{P_0}{N_{\text{eff}}}\exp(-j\omega_0 t_0)\cdot\sum_{n=-\infty}^{\infty} R_{\text{sinc}}(n)R_p\left(\frac{t_0}{\tau}-\frac{n}{\Omega\tau}\right).$$

Proof: Since the bandwidth of $\operatorname{sinc}(\Omega t)$ is confined within $(-\Omega/2,\,\Omega/2)$, the bandwidth of $\operatorname{sinc}(\Omega t-a)\operatorname{sinc}(\Omega t-b)$ is confined within $(-\Omega,\,\Omega)$, where a and b are arbitrary constants. Thus, for $m \neq 0$, we have $\int_{-\infty}^{\infty}\operatorname{sinc}(\Omega t-a)\operatorname{sinc}(\Omega t-b)\exp(j2\pi m\Omega t)\,dt = 0$, which implies $\int_{-\infty}^{\infty} s_m(t)s_n^*(t+t_0)\,dt = 0$, unless $m=n$. Therefore, from (7) and *Lemma 2*, we have

$$\Omega\int_{-\infty}^{\infty} y_i(t)y_i^*(t+t_0)\,dt = P_0\Omega^2\exp(-j\omega_0 t_0)\int_{-\infty}^{\infty} G_1(t,\,t_0)\,dt = \frac{P_0}{N_{\text{eff}}}\exp(-j\omega_0 t_0)\sum_{n=-\infty}^{\infty} R_{\text{sinc}}(n)R_p\left(\frac{t_0}{\tau}-\frac{n}{\Omega\tau}\right).$$

■

Note that, from *Proposition 3*, we also have

$$\Omega\int_{-\infty}^{\infty} E\{y_i(t)\cdot y_i^*(t+t_0)\}\,dt = E\left\{\Omega\int_{-\infty}^{\infty} y_i(t)y_i^*(t+t_0)\,dt\right\} = \Omega\int_{-\infty}^{\infty} y_i(t)y_i^*(t+t_0)\,dt.$$

Lemma 3: If $\Omega\tau \ll 1$, we have: 1) $\Omega\int_{-\infty}^{\infty} G_1^2(t,\,t_0)\,dt \cong \alpha_2^2\tau^2 R_{\text{sinc}^2}(\Omega t_0)\sum_{n=-\infty}^{\infty} R_p^2((t_0/\tau)-(n/\Omega\tau))$; 2) $\Omega\int_{-\infty}^{\infty} G_2^2(t,\,t_0)\,dt \cong O(\tau^3)$; and 3) $\Omega\int_{-\infty}^{\infty} G_3(t,\,t_0)\,dt \cong O(\tau^4)$, where $O(\cdot)$ denotes "order of."

Proof: See Appendix B. ■

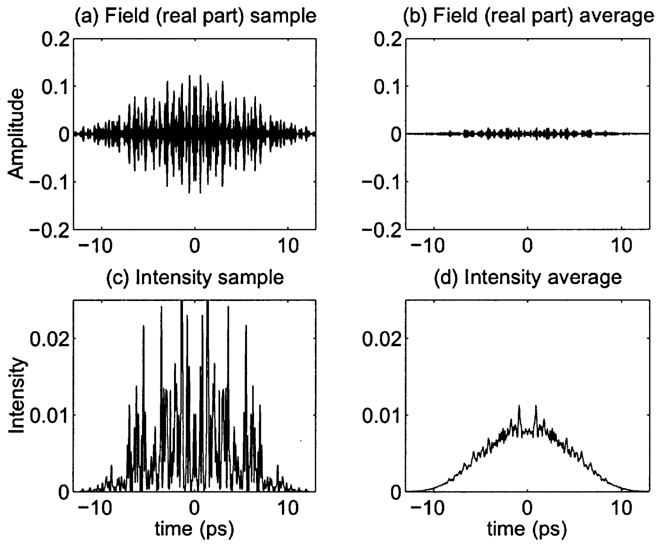

Fig. 2. Field and intensity of an encoded ULP. (a) Real part of the field (a sample). (b) Real part of the field (average). (c) Intensity (a sample). (d) Intensity (average).

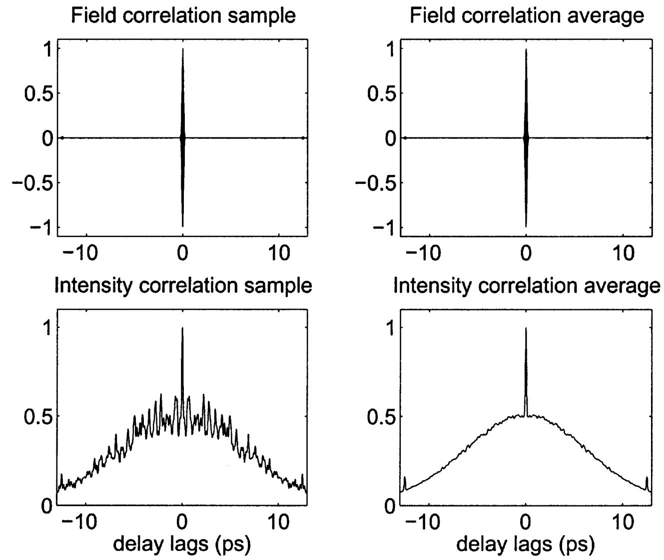

Fig. 3. Field and intensity correlation of an encoded ULP. (a) Real part of the field correlation (a sample). (b) Real part of the field correlation (average). (c) Intensity correlation (a sample). (d) Intensity correlation (average).

Proposition 4: If $\Omega\tau \ll 1$, the time-integrated intensity autocorrelation is approximated as

$$\Omega \int_{-\infty}^{\infty} E\{I_i(t)I_i(t+t_0)\}\,dt \cong \frac{P_0^2}{N_{\text{eff}}^2} R_{\text{sinc}^2}(\Omega t_0)\left\{1+\sum_{n=-\infty}^{\infty} R_p^2\left(\frac{t_0}{\tau}-\frac{n}{\Omega\tau}\right)\right\}. \quad (11)$$

Proof: Since $\Omega\tau \ll 1$, from *Lemma 1*, we have

$$\begin{aligned}\Omega \int_{-\infty}^{\infty} G_1(t,0)G_1(t+t_0,0)\,dt &\cong \alpha_2^2\tau^2\Omega\left(\sum_{n=-\infty}^{\infty} R_p\left(\frac{n}{\Omega\tau}\right)\right)^2 \int_{-\infty}^{\infty} \text{sinc}^2(\Omega t) \\ &\quad \cdot \text{sinc}^2(\Omega(t+t_0))\,dt \\ &\cong \alpha_2^2\tau^2 R_{\text{sinc}^2}(\Omega t_0). \end{aligned} \quad (12)$$

Thus, from *Proposition 2* and *Lemma 3*, we have

$$\begin{aligned}\Omega \int_{-\infty}^{\infty} E\{I_i(t)I_i(t+t_0)\}\,dt &\cong \frac{P_0^2}{N_{\text{eff}}^2} R_{\text{sinc}^2}(\Omega t_0) \\ &\quad \cdot\left\{1+\sum_{n=-\infty}^{\infty} R_p^2\left(\frac{t_0}{\tau}-\frac{n}{\Omega\tau}\right)+\frac{O(\tau^3)}{\tau^2}+\frac{O(\tau^4)}{\tau^2}\right\} \\ &\cong \frac{P_0^2}{N_{\text{eff}}^2} R_{\text{sinc}^2}(\Omega t_0)\left\{1+\sum_{n=-\infty}^{\infty} R_p^2\left(\frac{t_0}{\tau}-\frac{n}{\Omega\tau}\right)\right\}. \end{aligned} \quad (13)$$

■

The interpretation of *Proposition 4* is as follows: for most of the time, the time-averaged intensity autocorrelation has a functional form of the autocorrelation function $R_{\text{sinc}^2}(\Omega t_0)$, which is symmetric about $t_0 = 0$ with a peak autocorrelation value of $R_{\text{sinc}^2}(0) = \int_{-\infty}^{\infty} \text{sinc}^4(t)\,dt = 2/3$, decreases monotonically to zero, and its duration is approximately $2/\Omega$; however, it is doubled periodically at $t_0 = n/\Omega$ due to the second term in the parenthesis of the right-hand side of (13), where the intensity profile of the input ULP reappears. This follows from the fact that the intensity samples separated by t_0 are correlated when t_0 is within the vicinity (roughly $\pm\tau$) of integer multiples of $1/\Omega$, in which the periodicity comes from the spectral chip bandwidth. Note that the time-averaged field and intensity autocorrelations of the encoded waveforms yield measurements of the input ULP autocorrelation function $R_p(t/\tau)$, which is considered a difficult task.

Computer simulations were performed to corroborate the findings of the statistical properties. We used a Gaussian pulse shape given by $p_u(t) = \exp(-(2\ln 2)t^2)$. The simulation parameters were conducted for a $\tau = 100$ fs pulse and a spectral chip bandwidth of $\Omega = 80$ GHz. Expectation values were approximated by averaging over 100 trials. Figs. 2 and 3 summarize the computer simulation results, which match quite well to *Proposition 1*, *Corollary 1*, and *Propositions 3* and *4*. Using the simulation parameters, $\alpha_2 = \sqrt{\pi/4\ln 2}$ and the effective number of spectral chips is $N_{\text{eff}} = 117.4$.

III. System Model

The transmitter and receiver scheme for the hybrid PPM/ULP-CDMA system considered in this paper are shown in Fig. 4. An ULP from a laser source is shifted into one of the M possible signal locations with separation T_{ps} according to the data symbol with symbol period T_s, and is CDMA encoded with its unique spectral filter. A decoding filter at the receiver despreads the encoded signal back to a ULP, and the pulse position is detected through a photo detector array at the output of the time–space processor, which linearly converts the finite-length (determined by the time window of the time–space processor) interval of the incoming temporal signal, at the instant determined by a reference pulse, into the corresponding spatial image. More detailed discussion on the time–space processor will be given in Part II. Finally, decision circuitry selects the symbol with the largest intensity, and then

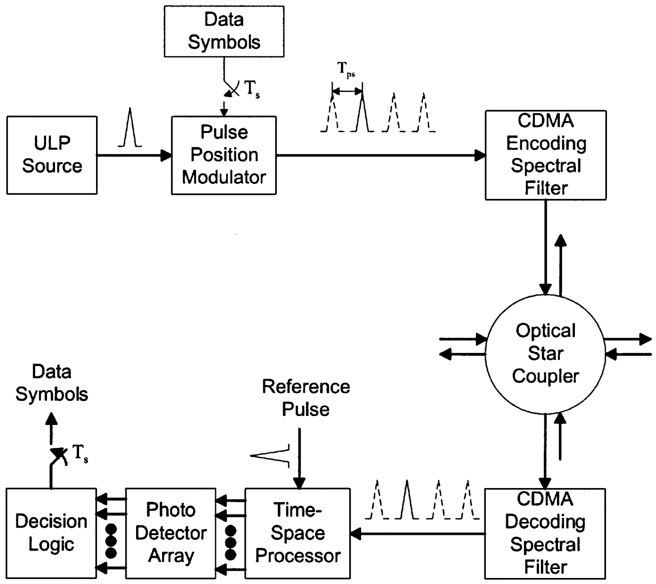

Fig. 4. Transmitter/receiver scheme of the PPM/ULP-CDMA system.

the transmitted information is extracted from the detected pulse position.

In order to convert a CDMA-decoded ULP to a spatial signal on the detector array, a timing reference is required, as mentioned above. Since femtosecond-scale time synchronization between transmitter and receiver is difficult, it must be extracted from the transmitted signals. Sending a CDMA-encoded reference pulse along with the data is one possible solution. A second solution is to use previous data as a reference for the current pulse position, together with an initial setup period. However, in Part I of this paper, we assume that a perfect time reference at the receiver is available by some means. Practical implementations and their effects on the performance of the proposed system will be considered in Part II.

Now, consider the signal at the desired user's receiver. In the following analysis, we will consider only interuser interference, as it is the dominant source of degradation except at low signal-to-noise ratio (SNR). Let λ_j be the time delay of the jth interferer, including the effect of the PPM. Then, the received signal is

$$r(t) = y_d(t) + \sum_{j=1}^{J-1} y_j(t-\lambda_j) \tag{14}$$

where $y_d(t)$ is the desired user's encoded signal and J is the number of users. Here, we assume that λ_j is uniform over a symbol period, while the time delay of the desired user is set to zero without loss of generality. After passing through the CDMA decoder, the desired user's signal despreads into a ULP, while the interfering signals remain spread out in time. Since we assumed random binary spreading sequences on all users, the statistical properties of a falsely decoded (interference) signal are the same as those of an encoded signal.

Proposition 5: As $N_{\text{eff}} \to \infty$, $e_i(t) \triangleq \sqrt{N_{\text{eff}}} y_i(t) \exp(-j\omega_0 t)$ converges to a nonstationary complex Gaussian process with mean 0 and time-varying variance $P_0 \operatorname{sinc}^2(\Omega t)$. In addition, if t is not an integer multiple of $\frac{1}{2\Omega}$, the variances of its real and imaginary parts are equal.

Proof: See Appendix C. ■

By *Proposition 5*, we can approximate the complex envelope of an interference signal, for a given λ_j, as a nonstationary complex Gaussian process with mean zero and equal time-varying variances of its real and imaginary parts given by $(P_0/2N_{\text{eff}}) \operatorname{sinc}^2(\Omega(t-\lambda_j))$, when N_{eff} is sufficiently large.

Now consider the correlation characteristics. Since PPM with pulse separation T_{ps} is employed, the time differences between interference samples of interest are mT_{ps}, $m = 1, \ldots, M-1$. Since $\Omega\tau \ll 1$, we can set T_{ps} sufficiently greater than τ but sufficiently smaller than $1/M\Omega$. Then, $R_p((mT_{\text{ps}}/\tau) - (n/\Omega\tau)) \cong 0$ for $m = 1, \ldots, M-1$ and any integer n. Thus, $E\{y_i(t)y_i^*(t + mT_{\text{ps}})\} \cong 0$ from *Proposition 1* and *Lemma 1*. Therefore, the interference samples can be assumed uncorrelated, which implies mutual independence since they are Gaussian.

IV. Performance Analysis and Numerical Evaluation

In this section, we will analyze the performance of the proposed hybrid PPM/ULP-CDMA system. To facilitate the analysis, we will assume that the intensity samples are taken instantaneously at the possible pulse positions and the detection process is to choose the largest one. Let us define

$$y(t;\boldsymbol{\lambda}) \triangleq \sum_{j=1}^{J-1} y_j(t-\lambda_j) \tag{15}$$

where $\boldsymbol{\lambda} = (\lambda_1, \ldots, \lambda_{J-1})$. Then, for fixed t and $\boldsymbol{\lambda}$, $y(t;\boldsymbol{\lambda})$ is a complex Gaussian random variable with mean zero and the variances of its real and imaginary parts given by $\sigma^2(t;\boldsymbol{\lambda})$, where $\sigma^2(t;\boldsymbol{\lambda}) = \sum_{j=1}^{J-1} \sigma_j^2(t;\lambda_j)$ and

$$\sigma_j^2(t;\lambda_j) = \frac{P_0}{2N_{\text{eff}}} \operatorname{sinc}^2(\Omega(t-\lambda_j)).$$

Let I_d and I_r be the intensities sampled at the desired signal location ($t = 0$), and another signal location which is rT_{ps} apart from the desired slit ($|t| = rT_{\text{ps}}$), respectively. Due to the symmetry of the $\operatorname{sinc}^2(\cdot)$ and the probability density function (pdf) of $\boldsymbol{\lambda}$, we can assume that $t \geq 0$ without loss of generality. Then, the conditional pdfs of I_r and I_d are [20]

$$f_r(I_r|\boldsymbol{\lambda}) = \begin{cases} \dfrac{1}{2\sigma^2(rT_{\text{ps}};\boldsymbol{\lambda})} \exp\left(-\dfrac{I_r}{2\sigma^2(rT_{\text{ps}};\boldsymbol{\lambda})}\right) & \sigma^2(rT_{\text{ps}},\boldsymbol{\lambda}) > 0 \\ \delta(I_r) & \sigma^2(rT_{\text{ps}},\boldsymbol{\lambda}) = 0 \end{cases} \tag{16}$$

and

$$f_d(I_d|\boldsymbol{\lambda}) = \begin{cases} \dfrac{1}{2\sigma^2(0;\boldsymbol{\lambda})} \exp\left(-\dfrac{(P_0+I_d)}{2\sigma^2(0;\boldsymbol{\lambda})}\right) \mathrm{I}_0\left(\dfrac{\sqrt{P_0 I_d}}{\sigma^2(0;\boldsymbol{\lambda})}\right) & \sigma^2(0;\boldsymbol{\lambda}) > 0 \\ \delta(I_d - P_0) & \sigma^2(0;\boldsymbol{\lambda}) = 0 \end{cases} \tag{17}$$

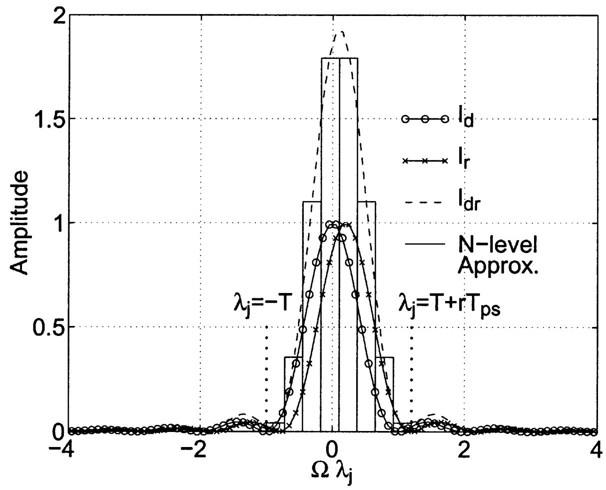

Fig. 5. N-level approximation.

respectively, where $\mathrm{I}_0(\cdot)$ is the zeroth-order modified Bessel function of the first kind. Let

$$l_d \triangleq \frac{2N_{\rm eff}\sigma^2(0;\,\boldsymbol{\lambda})}{P_0}$$

and

$$l_r \triangleq \frac{2N_{\rm eff}\sigma^2(rT_{\rm ps};\,\boldsymbol{\lambda})}{P_0}$$

be the effective number of interferers (i.e., interference variance $2\sigma^2$ normalized by the peak variance, $P_0/N_{\rm eff}$, of a single interferer) at the desired location and the one separated by $rT_{\rm ps}$ seconds, respectively. Then the following proposition holds:

Proposition 6: The pairwise probability, conditioned on $l_d + l_r$, is

$$\Pr\{I_d < I_r | l_d + l_r = l\} = \frac{1}{2}\exp\left(-\frac{N_{\rm eff}}{l}\right), \qquad l > 0. \quad (18)$$

Proof: See Appendix D. ■

From the conditional pairwise error probability, we get the unconditional pairwise error probability as

$$\Pr\{I_d < I_r\} = E\{\Pr\{I_d < I_r | l_d + l_r\}\}. \quad (19)$$

To evaluate (19), the pdf of $l_d + l_r$ must be known. Since l_d and l_r are functions of $\boldsymbol{\lambda}$, in principle, it could be obtained from the pdf of $\boldsymbol{\lambda}$. However, there does not appear to be a way of obtaining the pdf in closed form. Thus, we will use three methods to evaluate (19). The first two are numerical evaluations based on approximations of the pdf of $l_d + l_r$ obtained by truncating the $\mathrm{sinc}^2(\cdot)$ function in the time-varying variance, and will be described later; the other is an N-level approximation shown in Fig. 5. Note that a two-valued approximation was successfully used to approximate Gaussian interference with a randomly varying variance in [21]. The N-level approximation is obtained by quantizing the $\mathrm{sinc}^2(\cdot)$ function with an N-level function, and can be described as follows:

- Let

$$l_d(\lambda_j) = \frac{2N_{\rm eff}\sigma_j^2(0;\,\lambda_j)}{P_0}$$

and

$$l_r(\lambda_j) = \frac{2N_{\rm eff}\sigma_j^2(rT_{\rm ps};\,\lambda_j)}{P_0}.$$

- Assume that $l_{dr}(\lambda_j) = l_d(\lambda_j) + l_r(\lambda_j) = 0$ unless $\lambda_j \in [-T,\, T + rT_{\rm ps}]$, where $T \triangleq 1/\Omega$, which is the minimum interval that contains the mainlobes of both $l_d(\lambda_j)$ and $l_r(\lambda_j)$ (see Fig. 5). This approximation helps reduce the region of $\boldsymbol{\lambda}$ of interest and will be justified later.
- Let z_q^r, $q = 1, \ldots, 2N$, be the interval

$$\left[-T + \frac{(q-1)(2T + rT_{\rm ps})}{2N},\, -T + \frac{q(2T + rT_{\rm ps})}{2N}\right]$$

and $\zeta_q^r = 2N/(2T + rT_{\rm ps}) \int_{z_q^r} l_{dr}(\lambda_j)\, d\lambda_j$. In other words, the z_q^r are equal-length intervals that span the region of interest ($[-T,\, T + rT_{\rm ps}]$) and $\zeta_q^r = E\{l_{dr}(\lambda_j) | \lambda_j \in z_q^r\}$ is the average value of $l_{dr}(\lambda_j)$ within the interval z_q^r. Then, we approximate $l_{dr}(\lambda_j)$ as ζ_q^r if $\lambda_j \in z_q^r$.

Then, it is seen that $\zeta_q^r = \zeta_{2N-q+1}^r$, $q = 1, \ldots, N$, due to the symmetry of the $\mathrm{sinc}^2(\cdot)$ function. The N-level approximation described above is a simple one, but may not be an optimal way to represent $l_{dr}(\lambda_j)$ with N values. However, it will be shown later that it yields a good approximation to the upper bound of the bit error probability.

The above approximation implies that interferers whose delays are not in $[-T,\, T + rT_{\rm ps}]$ can be assumed to have no effect on the desired user. Let us consider the case where the number of interferers within the delay interval $[-T,\, T + rT_{\rm ps}]$ is k. Then, the probability of this event is

$$P(r,\, k) = \binom{J-1}{k}\left(\frac{2T + rT_{\rm ps}}{T_s}\right)^k \left(1 - \frac{2T + rT_{\rm ps}}{T_s}\right)^{J-k-1}. \quad (20)$$

In this case, each delay of the k users is within one of the z_q^r, $q = 1, \ldots, 2N$, equiprobably. Thus, each l_{dr} of the k users can take one of the values $\zeta_1^r, \ldots, \zeta_N^r$ with equal probability $1/N$, while the other $J - 1 - k$ users do not interfere with the desired user at all. Let i_c be the number of interferers whose l_{dr} takes the value of ζ_c^r. Then, it is easily seen that $\sum_{n=1}^N i_n = k$, $l_d + l_r \approx \sum_{c=1}^N i_c \zeta_c^r$, and the probability of this event for a given k is $(k!/(i_1! \cdots i_N!))(1/N)^k$. Therefore, we can approximate (19) as

$$\Pr\{I_d < I_r\} \cong \sum_{k=1}^{J-1} P(r,\, k) P_s(r,\, k) \quad (21)$$

where

$$P_s(r,\, k) = \sum_{i_1 + \cdots + i_N = k} \frac{k!}{i_1! \cdots i_N!}\left(\frac{1}{N}\right)^k P_s(r,\, k | i_1, \ldots, i_N) \quad (22)$$

and

$$P_s(r,\, k | i_1, \ldots, i_N) = \frac{1}{2}\exp\left(-\frac{N_{\rm eff}}{\sum_{c=1}^N i_c \zeta_c^r}\right). \quad (23)$$

Note that (21) is a function of r. There are $M(M-1)$ ways of choosing the positions of the desired and interfering user from M possible positions. Among them, the number of $rT_{\rm ps}$-apart signal position pairs is $2(M - r)$. By assuming equiprobable

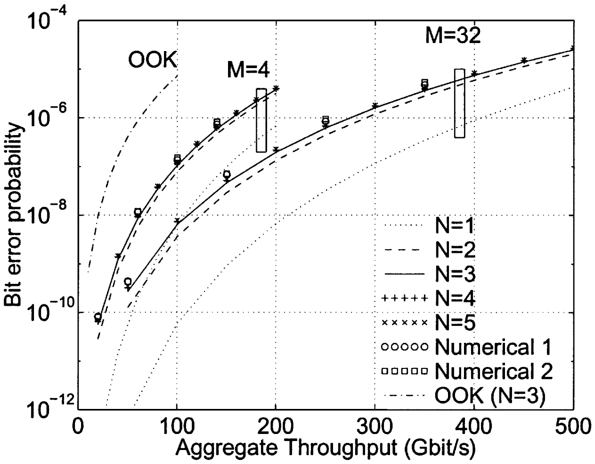

Fig. 6. Bit error probabilities when $\tau = 200$ fs and $N_{\rm eff} = 94$.

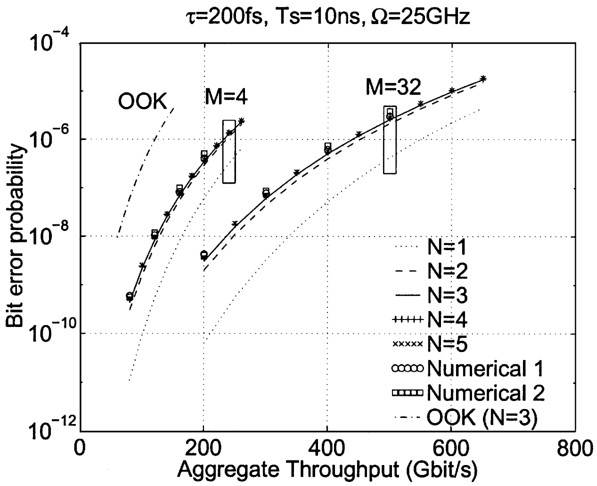

Fig. 7. Bit error probabilities when $\tau = 200$ fs and $N_{\rm eff} = 188$.

information symbols, we get the union bound on the symbol error probability as

$$P_s \leq \sum_{r=1}^{M-1} \frac{2(M-r)}{M} \Pr\{I_d < I_r\}. \tag{24}$$

Let $b(r)$ be the average number of bit errors per the number of bits in a symbol, caused by falsely detecting a symbol that is $rT_{\rm ps}$-apart from the desired symbol. Then, we get the union bound on the bit error probability as

$$P_b \leq \sum_{r=1}^{M-1} \frac{2(M-r)}{M} b(r) \Pr\{I_d < I_r\}. \tag{25}$$

Note that $b(r)$ depends on the mapping rule of binary digits into PPM symbols. In the following numerical evaluations, Gray encoding is assumed.

In Figs. 6 and 7, the union bound on the bit error probabilities of the proposed hybrid PPM/ULP-CDMA system are shown for $N = 1, \ldots, 5$ when $p_u(t) = \exp(-(2\ln 2)t^2)$, $\tau = 200$ fs, $T_{\rm ps} = 400$ fs, $M = 32$, and $\Omega = 50$ GHz ($T = 20$ ps, $N_{\rm eff} = 94$) and $\Omega = 25$ GHz ($T = 40$ ps, $N_{\rm eff} = 188$). The results from numerical method 1 are also based on (21). For a given k, however, instead of using (22), we generate λ_j with a uniform distribution over $[-T, T + rT_{\rm ps}]$ and evaluate

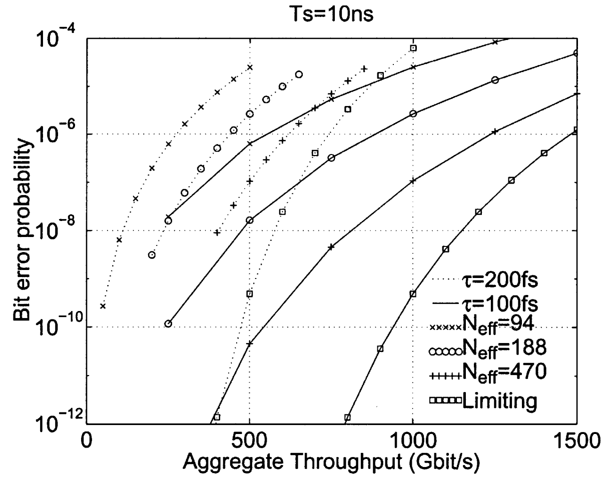

Fig. 8. Bit error probabilities when $\tau = 100$ fs and $\tau = 200$ fs.

$l_d(\lambda_j) = \mathrm{sinc}^2(\Omega\lambda_j)$ and $l_r(\lambda_j) = \mathrm{sinc}^2(\Omega(rT_{\rm ps} - \lambda_j))$. Then, $P_s(r, k)$, at a given l_d and l_r, is evaluated from *Proposition 6*. Finally, we evaluate the pairwise bit error probability by averaging each result of 20 000 runs obtained from (21). Note that the truncated $\mathrm{sinc}^2(\cdot)$ function used in numerical method 1 contains only the mainlobe. The numerical method 2 is identical to numerical method 1, except that it uses the largest sidelobe as well as the mainlobe. In other words, λ_j is generated with a uniform distribution over $[-2T, 2T + T_{\rm ps}]$ and (20) is modified as

$$P(r,k) = \binom{J-1}{k} \left(\frac{4T + rT_{\rm ps}}{T_s}\right)^k \left(1 - \frac{4T + rT_{\rm ps}}{T_s}\right)^{J-k-1}.$$

The performance of the ULP-CDMA system using OOK [4], with the same T_s, τ, and Ω, is also plotted for comparison. We slightly modify the bit error probability given in [4], by taking the sinc-square form of the time-varying variance of the encoded pulse, which was simplified to a rectangular one in [4], into account.

From the numerical results, we see that the results of method 1 are quite close to those of method 2. Thus, it appears to be justified to ignore the sidelobes of the $\mathrm{sinc}^2(\cdot)$ functions in the analysis. It is observed that the results from the N-level approximation match those obtained from the numerical methods quite well for the two cases. Indeed, $N \geq 3$ is shown to be sufficient to get a good approximation for the two cases. From the results, it is clearly seen that the aggregate throughput of the PPM/ULP-CDMA system is much higher than that of the ULP-CDMA system with OOK, and that the performance of the proposed system gets better as the effective number of chips, $N_{\rm eff}$, increases. It is also seen that the bandwidth efficiency of the proposed system gets better as M increases.

In Fig. 8, the union bound for the bit error probabilities of the proposed hybrid PPM/ULP-CDMA system are shown for $\Omega = 100$ GHz ($T = 10$ ps, $N_{\rm eff} = 94$), $\Omega = 50$ GHz ($T = 20$ ps, $N_{\rm eff} = 188$), and $\Omega = 20$ GHz ($T = 50$ ps, $N_{\rm eff} = 470$), when $p_u(t) = \exp(-(2\ln 2)t^2)$, $\tau = 100$ fs, $T_{\rm ps} = 200$ fs, $M = 32$, respectively. The N-level approximation with $N = 3$ is used for the evaluation. The results shown in Figs. 6 and 7, with $M = 32$, are replotted for comparison. We can see that we improve the performance of the proposed system by reducing the ULP duration τ while the spectral chip bandwidth remains constant (therefore, the effective number of chips increases). This is due to the enlarged bandwidth by reducing the ULP duration. It is also seen that we can improve the performance of the proposed system by reducing τ while the effective number of chips remains constant (therefore, the spectral chip bandwidth increases). This is also primarily due to the enlarged bandwidth. It indicates that, for a fixed effective number of chips (i.e., $\tau\Omega$ is a constant), smaller τ (and larger Ω) yields better performance because the duration of an interfering signal is reduced, but yet has the same peak power reduction.

Now, consider the effect when we increase the number of spectral chips with a fixed bandwidth. As N_{eff} increases, the duration T of an encoded pulse increases, while the power of each interferer decreases. Thus, the number of effective interferers (those that put significant energy in the time window mainlobe of the desired user), also increases. Then, the interference can be approximated as a stationary complex Gaussian process with variance $(P_0/N_{\text{eff}})((J-1)/\Omega T_s) = (\alpha_2(J-1)P_0\tau/T_s)$, in part by invoking the central limit theorem. In this case, the SNR per symbol is $\gamma_s = T_s/\alpha_2\tau(J-1) \approx \log_2 M/\alpha_2\tau\kappa$, where $\kappa = J\log_2 M/T_s$ is the aggregate throughput. Since the pdf of the actual interference has a more impulsive nature (i.e., a heavier tail) than the Gaussian process, the performance obtained by the above approximation provides the limiting achievable one (also plotted in Fig. 8) for the proposed system. Thus, the limiting performance is given by the following proposition.

Proposition 7: Let P_{req} be the required bit error probability. Then, the limiting aggregate throughput and the bandwidth efficiency are given by

$$\kappa_{\text{lim}} \cong \frac{\log_2 M}{2\alpha_2\tau(\ln M - \ln(4P_{\text{req}}))}$$

and

$$\beta_{\text{lim}} \cong \frac{\log_2 M}{2\alpha_2 B(\ln M - \ln(4P_{\text{req}}))}$$

respectively.

Proof: Since the union bound for the bit error probability of M-ary orthogonal modulation/noncoherent reception in an additive white Gaussian noise (AWGN) channel is $(M/4)e^{-(\gamma_s/2)} = (M/4)e^{-(\log_2 M/2\alpha_2\tau\kappa)}$ [20], we have $\kappa_{\text{lim}} \cong \log_2 M/\alpha_2\tau\gamma_{\text{req}}$, where $\gamma_{\text{req}} = 2(\ln M - \ln(4P_{\text{req}}))$. The remaining part is straightforward, since the FWHM bandwidth of $P(\omega) = P_u(\tau\omega)$ is B/τ. ∎

For example, $p_u(t) = \exp(-(2\ln 2)t^2)$, $M = 32$, $\tau = 100$ fs, and $P_{\text{req}} = 10^{-6}$ results in $\kappa_{\text{lim}} = 1.48$ Tb/s and $\beta_{\text{lim}} = 0.335$ bps/Hz. When $P_{\text{req}} = 10^{-9}$, κ_{lim} and β_{lim} are reduced to 1 Tb/s and 0.233 bps/Hz, respectively. In Fig. 9, the maximum achievable throughput, κ_{lim}, is plotted as a function of M, showing that we can improve the performance by increasing M.

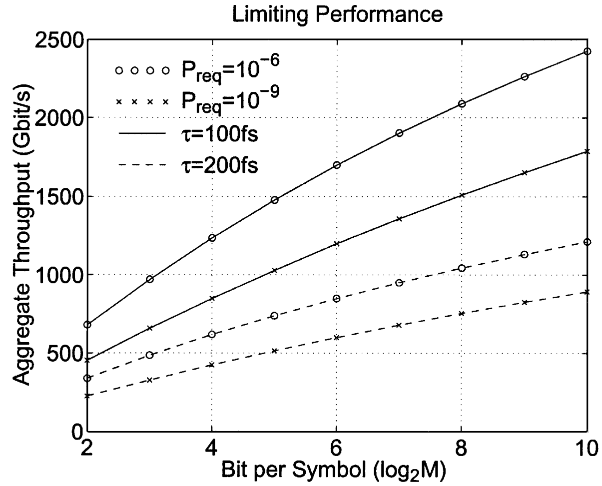

Fig. 9. Limiting aggregate throughput κ_{lim} for $P_{\text{req}} = 10^{-6}$ and 10^{-9} when $\tau = 100$ fs and $\tau = 200$ fs.

V. Concluding Remark

In this paper, a hybrid PPM/ULP-CDMA system was proposed to efficiently exploit the large bandwidth of the optical fiber channels. The proposed hybrid PPM/ULP-CDMA system employed the PPM with very short pulse separation by virtue of the time–space processing technique in [16], while conventional PPM/ULP-CDMA systems used PPM pulse separations comparable to a CDMA encoded signal duration. Thus, the bandwidth efficiency of the proposed system could be much higher than those of the conventional PPM/ULP-CDMA systems.

The statistical properties of a CDMA-encoded ULP, previously done for a simple rectangular pulse assumption in [4], were investigated based on a general ULP model. The pseudonoise characteristics of an encoded ULP was again confirmed with the general ULP model. A set of computer simulations was performed to corroborate the derived statistical properties in the case of an encoded Gaussian-shaped ULP. It was shown that, with the general ULP model, the peak power of an encoded ULP was reduced not by the number of chips as in [4], but by the effective number of chips that was determined by the ULP duration, the ULP pulse shape, and the spectral chip bandwidth. It was also shown that the encoded ULP could be well approximated to a nonstationary complex Gaussian process with time-varying variance.

Through the analysis of the proposed hybrid PPM/ULP-CDMA system, the N-level approximation method was used to evaluate the union bound on the bit error probability of the proposed system. It was shown that the N-level approximation with $N \geq 3$ could provide results close to those obtained from numerical methods. For comparison, the performance of the proposed hybrid PPM/ULP-CDMA system was plotted against that of the ULP-CDMA system using OOK. From our results, it was shown that we can improve the performance of the ULP-CDMA system substantially by employing PPM. It was also shown that increasing the effective number of chips, the possible signal positions in PPM, or the bandwidth, could provide better performance.

In order to investigate the performance limit of the proposed hybrid PPM/ULP-CDMA system, the case of a very large number of effective chips and a very large number of users was considered. In this case, the interference was approximated as a stationary complex Gaussian random process, and the limiting aggregate throughput and the bandwidth efficiency were derived as functions of the number of possible signal positions M in PPM and the required bit error probability.

The limiting achievable aggregate throughput was up to 1.5 Tb/s and 1 Tb/s with $\tau = 100$ fs ULP and $M = 32$ PPM at $P_{\rm req} = 10^{-6}$ and 10^{-9}, respectively. In addition, it can be further improved by increasing the number of possible signal positions M in PPM, theoretically up to the ratio of the symbol period to the ULP duration.

APPENDIX A
PROOF OF *PROPOSITION 2*

The intensity autocorrelation is given by

$$E\{I_i(t)I_i(t+t_0)\} = P_0^2\Omega^2 \sum_k \sum_l \sum_m \sum_n \cdot E\left\{a_k^{(i)} a_l^{(i)} a_m^{(i)} a_n^{(i)}\right\} s_k(t)s_l^*(t)s_m(t+t_0)s_n^*(t+t_0). \tag{26}$$

The expectation of the product of the four code elements is nonzero for the following cases: a) when $k = l = m = n$, then $E\{a_k^4\} = 1$; b) when $k = l \neq m = n$, then $E\{a_k^2 a_m^2\} = E\{a_k^2\}E\{a_m^2\} = 1$; c) when $k = m \neq l = n$, then $E\{a_k^2 a_l^2\} = E\{a_k^2\}\, E\{a_l^2\} = 1$; d) when $k = n \neq l = m$, then $E\{a_k^2 a_l^2\} = E\{a_k^2\}\, E\{a_l^2\} = 1$. In case a), we have $\sum_k |s_k(t)|^2 |s_k(t+t_0)|^2 = G_3(t, t_0)$. The double summation term in cases a) and b) can be combined to yield $\sum_k \sum_m |s_k(t)|^2 |s_m(t+t_0)|^2 = G_1(t, 0)G_1(t+t_0, 0)$, where the double summation is separable. Similarly, cases a) and c) are combined to yield $\sum_k \sum_l s_k(t)s_k(t+t_0)\, s_l^*(t)s_l^*(t+t_0) = |G_2(t, t_0)|^2$. Finally, cases a) and d) are combined to yield $\sum_k \sum_l s_k(t)s_k^*(t+t_0)\; s_l^*(t)s_l(t+t_0) = |G_1^2(t, t_0)|^2$. In addition, $G_1(t, t_0)$ and $G_2(t, t_0)$ are real as shown in (4) and (5). Therefore, we have $E\{I_i(t)I_i(t+t_0)\} \cong P_0^2\Omega^2 (G_1(t, 0)G_1(t+t_0, 0) + G_1^2(t, t_0) + G_2^2(t, t_0) - 2G_3(t, t_0))$.

APPENDIX B
PROOF OF *LEMMA 3*

1) Since $\Omega\tau \ll 1$, from *Lemma 1*, we have

$$\begin{aligned} G_1^2(t, t_0) &\cong \alpha_2^2\tau^2 \mathrm{sinc}^2(\Omega t)\mathrm{sinc}^2(\Omega(t+t_0)) \left(\sum_{n=-\infty}^{\infty} R_p\left(\frac{t_0}{\tau} - \frac{n}{\Omega\tau}\right)\right)^2 \\ &\cong \alpha_2^2\tau^2 \mathrm{sinc}^2(\Omega t)\mathrm{sinc}^2(\Omega(t+t_0)) \sum_{n=-\infty}^{\infty} R_p^2\left(\frac{t_0}{\tau} - \frac{n}{\Omega\tau}\right) \end{aligned} \tag{27}$$

where the last approximation follows from the finite duration of $R_p(\cdot)$. Thus, we have

$$\Omega \int_{-\infty}^{\infty} G_1^2(t, t_0)\, dt \cong \alpha_2^2\tau^2 R_{\mathrm{sinc}^2}(\Omega t_0) \sum_{n=-\infty}^{\infty} R_p^2\left(\frac{t_0}{\tau} - \frac{n}{\Omega\tau}\right).$$

2) Since $\Omega\tau \ll 1$, we have

$$G_2^2(t, t_0) \cong \alpha_2^2\tau^2 \mathrm{sinc}^2(\Omega t)\, \mathrm{sinc}^2(\Omega(t+t_0)) \cdot \sum_{n=-\infty}^{\infty} p_2^2\left(\frac{2t+t_0}{\tau} + \frac{n}{\Omega\tau}\right)$$

from *Lemma 1*. Thus, we have

$$\begin{aligned} \Omega \int_{-\infty}^{\infty} G_2^2(t, t_0)\, dt &\cong \alpha_2^2\tau^2\Omega \sum_{n=-\infty}^{\infty} \int_{-\infty}^{\infty} \mathrm{sinc}^2(\Omega t)\cdot \mathrm{sinc}^2(\Omega(t+t_0)) p_2^2 \cdot \left(\frac{2t+t_0}{\tau} + \frac{n}{\Omega\tau}\right) dt \\ &\cong \frac{\alpha_2^2\tau^2\Omega}{2} \sum_{n=-\infty}^{\infty} \left(\mathrm{sinc}^2\left(\frac{\Omega t_0}{2} + \frac{n}{2}\right) \mathrm{sinc}^2\left(\frac{\Omega t_0}{2} - \frac{n}{2}\right)\right) \cdot \int_{-\infty}^{\infty} p_2^2\left(\frac{t}{\tau}\right) dt = O(\tau^3) \end{aligned} \tag{28}$$

where the last equality follows by approximating $p_u(t/\tau)$ with $\alpha_1\tau\delta(t)$, so that

$$\begin{aligned} \int_{-\infty}^{\infty} p_2^2\left(\frac{t}{\tau}\right) dt &= \frac{1}{\alpha_2^2\tau^2} \int_{-\infty}^{\infty}\int_{-\infty}^{\infty}\int_{-\infty}^{\infty} p_\tau(\sigma_1)p_\tau(\sigma_2) \cdot p_\tau(t-\sigma_1)p_\tau(t-\sigma_2)\, d\sigma_1\, d\sigma_2\, dt \\ &= \frac{1}{\alpha_2\tau} \int_{-\infty}^{\infty}\int_{-\infty}^{\infty} p_\tau(\sigma_1)p_\tau(\sigma_2) \cdot R_p\left(\frac{\sigma_1 - \sigma_2}{\tau}\right) d\sigma_1\, d\sigma_2 \cong \frac{\alpha_1^2\tau}{\alpha_2}. \end{aligned} \tag{29}$$

3) We get $\Omega \int_{-\infty}^{\infty} G_3(t, t_0)\, dt \cong \Omega^2\alpha_1^4\tau^4\, \mathrm{sinc}^2(\Omega t)\, \mathrm{sinc}^2(\Omega(t+t_0)) = O(\tau^4)$ by approximating $p_\tau(t)$ with $\alpha_1\tau\delta(t)$ in (6).

APPENDIX C
PROOF OF *PROPOSITION 5*

Let us define

$$h_m^{(i)}(t) = \frac{a_m^{(i)}}{\alpha_2\tau} \int_{-\infty}^{\infty} p_\tau(t-\sigma)\, \mathrm{sinc}(\Omega\sigma)\cos(2\pi m\Omega\sigma)\, d\sigma$$

and

$$q_m^{(i)}(t) = \frac{a_m^{(i)}}{\alpha_2\tau} \int_{-\infty}^{\infty} p_\tau(t-\sigma)\, \mathrm{sinc}(\Omega\sigma)\sin(2\pi m\Omega\sigma)\, d\sigma.$$

Then, we have

$$e_i(t) = \sqrt{\frac{P_0}{N_{\rm eff}}} \sum_{m=-\infty}^{\infty} \left(h_m^{(i)}(t) + jq_m^{(i)}(t)\right).$$

From now on, we omit the superscript i for convenience. First, consider the real part, $h_m(t)$. Let $N = cN_{\rm eff}$ be an integer, where c is a positive constant. Define $f_n(t) \triangleq \sum_{m=-\infty}^{\infty} h_{2mN+n}(t)$. Then, $f_n(t)$, $n = -N+1, \ldots, N$ are zero mean mutually independent random variables with $\sum_{n=-N+1}^{N} f_n(t) = \sum_{-\infty}^{\infty} h_m(t)$. Let us define

$$\begin{aligned} b_n^h(t) &\triangleq E\{f_n^2(t)\} \\ &= E\left\{\sum_{m_1=-\infty}^{\infty}\sum_{m_2=-\infty}^{\infty} h_{2m_1N+n}(t)h_{2m_2N+n}(t)\right\} \end{aligned}$$

$$= \sum_{m=-\infty}^{\infty} v_{2mN+n}(t)$$

and

$$B_N^h(t) \triangleq \sum_{n=-N+1}^{N} b_n^h(t)$$

where

$$\begin{aligned} &v_{2mN+n}(t) \\ &\quad= \left(\frac{1}{\alpha_2 \tau} \int_{-\infty}^{\infty} p_\tau(t-\sigma)\,\mathrm{sinc}(\Omega\sigma) \right. \\ &\qquad\quad \left. \cdot \cos(2\pi(2mN+n)\Omega\sigma)\,d\sigma \right)^2 \\ &\quad= \frac{1}{2\alpha_2^2\tau^2} \int_{-\infty}^{\infty}\int_{-\infty}^{\infty} p_\tau(t-\sigma_1)p_\tau(t-\sigma_2)\,\mathrm{sinc}(\Omega\sigma_1) \\ &\qquad \cdot \mathrm{sinc}(\Omega\sigma_2)(\cos(2\pi(2mN+n)\Omega(\sigma_1+\sigma_2)) \\ &\qquad + \cos(2\pi(2mN+n)\Omega(\sigma_1-\sigma_2)))\,d\sigma_1\,d\sigma_2. \end{aligned} \tag{30}$$

By using the identity

$$\begin{aligned} &\sum_{m=-\infty}^{\infty} \cos(2\pi(2mN+n)\Omega\sigma) \\ &\quad= \cos(2\pi n\Omega\sigma) \sum_{m=-\infty}^{\infty} \cos(4\pi mN\Omega\sigma) \\ &\quad= \frac{1}{2N\Omega} \cos(2\pi n\Omega\sigma) \sum_{k=-\infty}^{\infty} \delta\left(\sigma + \frac{k}{2N\Omega}\right) \end{aligned}$$

we get

$$\begin{aligned} b_n^h(t) &= \frac{1}{4\alpha_2 c\tau} \sum_{k=-\infty}^{\infty} \int_{-\infty}^{\infty}\int_{-\infty}^{\infty} p_\tau(t-\sigma_1)p_\tau(t-\sigma_2) \\ &\quad \cdot \mathrm{sinc}(\Omega\sigma_1)\,\mathrm{sinc}(\Omega\sigma_2) \\ &\quad \cdot \left(\cos(2\pi n\Omega(\sigma_1-\sigma_2))\delta\left(\sigma_1 - \sigma_2 + \frac{k}{2N\Omega}\right) \right. \\ &\quad + \cos(2\pi n\Omega(\sigma_1+\sigma_2)) \\ &\quad \left. \cdot\, \delta\left(\sigma_1 + \sigma_2 + \frac{k}{2N\Omega}\right)\right) d\sigma_1\,d\sigma_2 \\ &= \frac{1}{4\alpha_2 c\tau} \sum_{k=-\infty}^{\infty} \cos\left(\frac{\pi nk}{N}\right) \int_{-\infty}^{\infty} \\ &\quad \cdot \left(p_\tau(t-\sigma)p_\tau\left(t-\sigma-\frac{k}{2N\Omega}\right)\mathrm{sinc}(\Omega\sigma) \right. \\ &\quad \cdot \mathrm{sinc}\left(\Omega\sigma + \frac{k}{2N}\right) + p_\tau(t-\sigma)p_\tau\left(t+\sigma+\frac{k}{2N\Omega}\right) \\ &\quad \left. \cdot \mathrm{sinc}(\Omega\sigma)\,\mathrm{sinc}\left(\Omega\sigma+\frac{k}{2N}\right)\right) d\sigma. \end{aligned} \tag{31}$$

Note that

$$\sum_{n=-N+1}^{N} \cos\left(\frac{\pi nk}{N}\right) = 2N \sum_{k'=-\infty}^{\infty} \delta_K(k-2k'N)$$

where $\delta_K(\cdot)$ is the Kronecker delta function. Thus, as $N_{\text{eff}} \to \infty$, we have

$$\begin{aligned} &\lim_{N_{\text{eff}}\to\infty} \frac{1}{N_{\text{eff}}} B_N^h(t) \\ &\quad= \lim_{N_{\text{eff}}\to\infty} \frac{1}{2\alpha_2\tau} \int_{-\infty}^{\infty} \sum_{k'=-\infty}^{\infty} \left(p_\tau(t-\sigma)p_\tau\left(t-\sigma-\frac{k'}{\Omega}\right) \right. \\ &\qquad \cdot \mathrm{sinc}(\Omega\sigma)\,\mathrm{sinc}(\Omega\sigma+k') + p_\tau(t-\sigma) \\ &\qquad \left. \cdot\, p_\tau\left(t+\sigma+\frac{k'}{\Omega}\right)\mathrm{sinc}(\Omega\sigma)\,\mathrm{sinc}(\Omega\sigma+k')\right) d\sigma \\ &\quad= \frac{1}{2}\mathrm{sinc}^2(\Omega t)\left(1 + p_2(0)\sum_{k'=-\infty}^{\infty} \delta_K\left(t - \frac{k'}{2\Omega}\right)\right) \end{aligned} \tag{32}$$

where the last equality follows from the fact that as

$N_{\text{eff}} \to \infty$,

$$\frac{1}{\alpha_2\tau} p_\tau(t-\sigma)p_\tau\left(t-\sigma-\frac{k'}{\Omega}\right) \to \delta(t-\sigma)\delta_K(k')$$

and

$$\begin{aligned} &\frac{1}{\alpha_2\tau} p_\tau(t-\sigma)p_\tau\left(t+\sigma+\frac{k'}{\Omega}\right) \to p_2(0)\delta(t-\sigma) \\ &\qquad \cdot\, \delta_K\left(t - \frac{k'}{2\Omega}\right) \end{aligned}$$

justified as follows. First, as $N_{\text{eff}} \to \infty$, $p_\tau(t-\sigma)$ gets concentrated at $\sigma = t$, which implies that

$$\frac{1}{\alpha_2\tau} p_\tau(t-\sigma)p_\tau\left(t-\sigma-\frac{k'}{\Omega}\right)$$

converges to a delta function when $k' = 0$, and vanishes otherwise. Since

$$\int_{-\infty}^{\infty} p_\tau^2(\sigma)\,d\sigma = \alpha_2\tau, \quad \frac{1}{\alpha_2\tau} p_\tau(t-\sigma)p_\tau\left(t-\sigma-\frac{k'}{\Omega}\right)$$

converges to $\delta(\sigma - t)\delta_K(k')$. Similarly, when

$$k' = -2\Omega t, \quad \frac{1}{\alpha_2\tau} p_\tau(t-\sigma)p_\tau\left(t+\sigma+\frac{k'}{\Omega}\right)$$

gets also concentrated at $\sigma = t$, and vanishes otherwise. Since

$$\int_{-\infty}^{\infty} p_\tau(\sigma)p_\tau(-\sigma)\,d\sigma = \alpha_2\tau p_2(0),$$

$$\frac{1}{\alpha_2\tau} p_\tau(t-\sigma)p_\tau\left(t+\sigma+\frac{k'}{\Omega}\right)$$

converges to $p_2(0)\delta(t-\sigma)\delta_K(t-(k'/2\Omega))$.

Now, define

$$\begin{aligned} c_n^h(t) &\triangleq E\left\{\left(f_n^h(t)\right)^4\right\} \\ &= \sum_{m_1=-\infty}^{\infty}\sum_{m_2=-\infty}^{\infty}\sum_{m_3=-\infty}^{\infty}\sum_{m_4=-\infty}^{\infty} E\left\{h_{2m_1N+n}(t)\right. \\ &\qquad \left. \cdot\, h_{2m_2N+n}(t)h_{2m_3N+n}(t)h_{2m_4N+n}(t)\right\} \end{aligned}$$

and $C_N^h(t) \triangleq \sum_{n=-N+1}^{N} c_n^h(t)$. As in Appendix A, only the $m_1 = m_2$ and $m_3 = m_4$, or $m_1 = m_3$ and $m_2 = m_4$, or $m_1 = m_4$ and $m_2 = m_3$ terms are nonzero. Since the three cases yield the same result, we have

$$\begin{aligned} c_n^h(t) &= 3\sum_{m_1=-\infty}^{\infty}\sum_{m_2=-\infty}^{\infty} h_{2m_1N+n}^2(t)h_{2m_2N+n}^2(t) \\ &\quad -2\sum_{m=-\infty}^{\infty} h_{2mN+n}^4(t) \le 3\left(b_n^h(t)\right)^2. \end{aligned} \tag{33}$$

By squaring (31), we have a double integral and a double summation, in which there are four terms. The first term, T_1, may be expressed as

$$T_1 = \frac{1}{32c^2\alpha_2^2\tau^2}\sum_{k_1=-\infty}^{\infty}\sum_{k_2=-\infty}^{\infty}\int_{-\infty}^{\infty}\int_{-\infty}^{\infty} p_\tau(t-\sigma_1)p_\tau(t-\sigma_2) \cdot p_\tau\left(t-\sigma_1-\frac{k_1}{2N\Omega}\right)p_\tau\left(t-\sigma_2-\frac{k_2}{2N\Omega}\right)\mathrm{sinc}(\Omega\sigma_1) \cdot \mathrm{sinc}\left(\Omega\sigma_1+\frac{k_1}{2N}\right)\mathrm{sinc}(\Omega\sigma_2)\,\mathrm{sinc}\left(\Omega\sigma_2+\frac{k_2}{2N}\right) \cdot\left(\cos\left(\frac{\pi n(k_1+k_2)}{N}\right)+\cos\left(\frac{\pi n(k_1-k_2)}{N}\right)\right)d\sigma_1\,d\sigma_2. \tag{34}$$

By taking the summation on the first cosine term over $n = -N+1$ to N and dividing it by N_{eff}, we get

$$\frac{1}{N_{\mathrm{eff}}}\sum_{n=-N+1}^{N}\cos\left(\frac{\pi n(k_1+k_2)}{N}\right) = 2c\sum_{k'=-\infty}^{\infty}\delta_K(k_1+k_2+2k'N). \tag{35}$$

Similarly, the second cosine term yields the same result except that the argument of the delta function is $k_1-k_2+2k'N$. Then, we have

$$T_1 = \frac{1}{16c\alpha_2^2\tau^2}\sum_{k_1=-\infty}^{\infty}\sum_{k'=-\infty}^{\infty}\int_{-\infty}^{\infty}\int_{-\infty}^{\infty} \cdot\Bigg[p_\tau(t-\sigma_1)p_\tau(t-\sigma_2)p_\tau\left(t-\sigma_1-\frac{k_1}{2N\Omega}\right) \cdot p_\tau\left(t-\sigma_2-\frac{k_1+2k'N}{2N\Omega}\right) \cdot \mathrm{sinc}(\Omega\sigma_1)\,\mathrm{sinc}\left(\Omega\sigma_1+\frac{k_1}{2N}\right)\mathrm{sinc}(\Omega\sigma_2) \cdot \mathrm{sinc}\left(\Omega\sigma_2+\frac{k_1+2k'N}{2N}\right)+p_\tau(t-\sigma_1)p_\tau(t-\sigma_2) \cdot p_\tau\left(t-\sigma_1-\frac{k_1}{2N\Omega}\right)p_\tau\left(t-\sigma_2+\frac{k_1+2k'N}{2N\Omega}\right) \cdot \mathrm{sinc}(\Omega\sigma_1)\,\mathrm{sinc}\left(\Omega\sigma_1+\frac{k_1}{2N}\right)\mathrm{sinc}(\Omega\sigma_2) \cdot \mathrm{sinc}\left(\Omega\sigma_2-\frac{k_1+2k'N}{2N}\right)\Bigg]d\sigma_1\,d\sigma_2. \tag{36}$$

Now, consider the function

$$\frac{1}{(\alpha_2\tau)^2}\,p_\tau(t-\sigma_1)p_\tau\left(t-\sigma_1-\frac{k_1}{2N\Omega}\right) \cdot p_\tau(t-\sigma_2)p_\tau\left(t-\sigma_2\pm\left(\frac{k_1}{2N\Omega}+\frac{k'}{\Omega}\right)\right).$$

As $N_{\mathrm{eff}}\to\infty$, similar to what was discussed earlier, the second half of the function, namely

$$p_\tau(t-\sigma_2)p_\tau\left(t-\sigma_2\pm\left(\frac{k_1}{2N\Omega}+\frac{k'}{\Omega}\right)\right)$$

gets concentrated at $\sigma_2 = t$ only when $(k_1/2N)+k'=0$ and vanishes otherwise. If $k'\neq 0$, $k_1=-2Nk'$ makes the first half, $p_\tau(t-\sigma_1)p_\tau\left(t-\sigma_1-(k_1/2N\Omega)\right)$, vanish. In addition, we have

$$\int_{-\infty}^{\infty} p_\tau(t-\sigma)p_\tau\left(t-\sigma\pm\frac{k_1}{2N\Omega}\right)d\sigma = \alpha_2\tau R_p\left(\frac{\alpha_2 k_1}{2c}\right).$$

Thus, it converges to $R_p^2(\alpha_2k_1/2c)\delta(t-\sigma_1)\,\delta(t-\sigma_2)\delta_K(k')$ as $N_{\mathrm{eff}}\to\infty$. Then, by substituting the delta function, we have

$$\begin{aligned}\lim_{N_{\mathrm{eff}}\to\infty}\frac{1}{N_{\mathrm{eff}}}\sum_{n=-N+1}^{N}T_1 &= \frac{1}{16c}\,\mathrm{sinc}^2(\Omega t)\sum_{k_1=-\infty}^{\infty}R_p^2\left(\frac{\alpha_2k_1}{2c}\right)\mathrm{sinc}\left(\Omega t+\frac{k_1}{2N}\right) \cdot\left(\mathrm{sinc}\left(\Omega t-\frac{k_1}{2N}\right)+\mathrm{sinc}\left(\Omega t+\frac{k_1}{2N}\right)\right)\\ &\leq \frac{1}{8c}\,\mathrm{sinc}^2(\Omega t)\sum_{k_1=-\infty}^{\infty}R_p^2\left(\frac{\alpha_2k_1}{2c}\right)<\infty\end{aligned} \tag{37}$$

where the last inequality follows from the fact that, from the definition of $p_u(t)$, there exists a positive function $\zeta(t)$ that is monotonically decreasing with respect to $|t|$ and is integrable, such that $R_p^2(\alpha_2k_1/2c)\leq\zeta(\alpha_2k_1/2c)$. Similarly, we can see that, as $N_{\mathrm{eff}}\to\infty$, the summation of the other remaining terms in the square of (31) over $n=-N+1$ to N, divided by N_{eff}, is finite by taking similar steps as in (34)–(37). Thus, we get $\lim_{N_{\mathrm{eff}}\to\infty}(1/N_{\mathrm{eff}})C_{cN\mathrm{eff}}<\infty$. Since $B_N(t)=0$ implies that $\sum_{m=-\infty}^{\infty}h_m(t)$ is identically zero, we can assume that $B_N(t)>0$ without loss of generality. Also, from (31), we have

$$b_n^h(t)\leq\frac{1}{4\alpha_2c}\sum_{k=-\infty}^{\infty}\int_{-\infty}^{\infty} \cdot\left(\left|p_u\left(\frac{t}{\tau}-\sigma\right)\right|\left|p_u\left(\frac{t}{\tau}-\sigma-\frac{\alpha_2k}{2c}\right)\right| +\left|p_u\left(\frac{t}{\tau}-\sigma\right)\right|\left|p_u\left(\frac{t}{\tau}+\sigma+\frac{\alpha_2k}{2c}\right)\right|\right)d\sigma.$$

Since $|p_u(\sigma)|$ is bounded by a positive function that is monotonically decreasing and integrable, we have

$$\sum_{k=-\infty}^{\infty}\left|p_u\left(\frac{t}{\tau}\pm\sigma\pm\frac{\alpha_2k}{2c}\right)\right|<\infty$$

which implies $b_n^h(t)<\infty$. Thus, we get $c_n^h(t)<\infty$. Finally, we have

$$\lim_{N_{\mathrm{eff}}\to\infty}\frac{C_{cN\mathrm{eff}}}{B_{cN_{\mathrm{eff}}}^2} = \lim_{N_{\mathrm{eff}}\to\infty} \cdot\frac{\left(\frac{1}{N_{\mathrm{eff}}}\right)\left(\frac{1}{N_{\mathrm{eff}}}C_{cN\mathrm{eff}}\right)}{\left(\frac{1}{N_{\mathrm{eff}}}B_{cN_{\mathrm{eff}}}\right)^2}=0 \tag{38}$$

which shows that, as $N_{\mathrm{eff}}\to\infty$, $\mathrm{Re}\{e_i(t)\}$ converges to a Gaussian process with mean zero and variance

$$\frac{P_0}{2}\,\mathrm{sinc}^2(\Omega t)\left(1+p_2(0)\sum_{n=-\infty}^{\infty}\delta_K\left(t-\frac{n}{2\Omega}\right)\right)$$

by the Lyapunov version of the central limit theorem [22]. Similarly, $\mathrm{Im}\{e_i(t)\}$ also converges to a Gaussian process with mean zero and variance

$$\frac{P_0}{2}\,\mathrm{sinc}^2(\Omega t)\left(1-p_2(0)\sum_{n=-\infty}^{\infty}\delta_K\left(t-\frac{n}{2\Omega}\right)\right).$$

As the last step, it can be shown that

$$\begin{aligned}
&E\left\{\mathrm{Re}\{e_i(t)\}\mathrm{Im}\{e_i(t+t_0)\}\right\}\\
&=\frac{P_0}{N_{\mathrm{eff}}}\sum_{m=-\infty}^{\infty}\sum_{n=-\infty}^{\infty}E\left\{h_m(t)q_n(t+t_0)\right\}\\
&=\frac{P_0}{\alpha_2^2\tau^2 N_{\mathrm{eff}}}\sum_{m=-\infty}^{\infty}\int_{-\infty}^{\infty}\int_{-\infty}^{\infty}p_\tau(t-\sigma_1)p_\tau(t+t_0-\sigma_2)\\
&\quad\cdot\mathrm{sinc}(\Omega\sigma_1)\,\mathrm{sinc}(\Omega\sigma_2)\cos(2\pi m\Omega\sigma_1)\\
&\quad\cdot\sin(2\pi m\Omega\sigma_2)\,d\sigma_1\,d\sigma_2=0
\end{aligned}\tag{39}$$

where the second equality follows the fact that $E\{a_m a_n\}=0$, for $m\neq n$, and the last equality follows the fact that $\cos(2\pi m\Omega\sigma_1)\sin(2\pi m\Omega\sigma_2)$ is an odd function of m. Thus, $e_i(t)$ converges to a complex Gaussian process with mean zero and variance $P_0\mathrm{sinc}^2(\Omega t)$. Finally, when t is not an integer multiple of $1/(2\Omega)$, $\sum_{n=-\infty}^{\infty}\delta_K\,(t-(n/2\Omega))=0$, which implies that the variances of its real and imaginary parts are equal, and given by $(P_0/2)\mathrm{sinc}^2(\Omega t)$.

APPENDIX D
PROOF OF *PROPOSITION 6*

From (16) and (17), we have

$$\begin{aligned}
\Pr\{I_d<I_r|\boldsymbol{\lambda}\}&=\frac{\sigma^2(rT_{\mathrm{ps}};\,\boldsymbol{\lambda})}{\sigma^2(0;\,\boldsymbol{\lambda})+\sigma^2(rT_{\mathrm{ps}};\,\boldsymbol{\lambda})}\\
&\quad\cdot\exp\left(-\frac{P_0}{2\sigma^2(0;\,\boldsymbol{\lambda})+2\sigma^2(rT_{\mathrm{ps}};\,\boldsymbol{\lambda})}\right)
\end{aligned}\tag{40}$$

for $\sigma^2(0;\,\boldsymbol{\lambda})+\sigma^2(rT_{\mathrm{ps}};\,\boldsymbol{\lambda})>0$. Note that the conditional probability depends on only the variances $\sigma^2(0;\,\boldsymbol{\lambda})$ and $\sigma^2(rT_{\mathrm{ps}};\,\boldsymbol{\lambda})$ for a given P_0. Thus, we can rewrite (40) as

$$\begin{aligned}
\Pr\{I_d<I_r|l_d,\,l_r\}&=\frac{l_r}{l_d+l_r}\exp\left(-\frac{N_{\mathrm{eff}}}{l_d+l_r}\right),\\
&\qquad l_d+l_r>0.
\end{aligned}\tag{41}$$

Therefore, we get

$$\begin{aligned}
&\Pr\{I_d<I_r|l_d+l_r=l\}\\
&\quad=E\{\Pr\{I_d<I_r|l_d,\,l_r\}|l_d+l_r=l\}\\
&\quad=\frac{E\{l_r|l_d+l_r=l\}}{l}\exp\left(-\frac{N_{\mathrm{eff}}}{l}\right),\qquad l>0
\end{aligned}$$

where $E\{l_r|l_d+l_r=l\}=l/2$ and is shown as follows. Without loss of generality, we can assume that the delays are uniform over a symbol period centered at $rT_{\mathrm{ps}}/2$. Let Q_l be the set of $\boldsymbol{\lambda}=(\lambda_1,\,\ldots,\,\lambda_{J-1})$ satisfying $\sum_{j=1}^{J-1}l_{dr}(\lambda_j)=l$. Then, for an element $\boldsymbol{\lambda}\in Q_l$, we define a collection $C(\boldsymbol{\lambda})=\{\tilde{\boldsymbol{\lambda}}=(\tilde\lambda_1,\,\ldots,\,\tilde\lambda_{J-1})|\tilde\lambda_j=\lambda_j$ or $rT_{\mathrm{ps}}-\lambda_j,\,j=1,\,\ldots,\,J-1\}\subset Q_l$. Note that, for any $\mathbf{q}\in C(\boldsymbol{\lambda})$, we get $C(\mathbf{q})=C(\boldsymbol{\lambda})$. Let us also define $a(\boldsymbol{\lambda})$ as the cardinality of $C(\boldsymbol{\lambda})$.

Since $\mathrm{sinc}^2(\cdot)$ is an even function, $l_d(\lambda_j)=l_r(rT_{\mathrm{ps}}-\lambda_j)$, which implies $l_{dr}(\lambda_j)=l_{dr}(rT_{\mathrm{ps}}-\lambda_j)$. Thus, we get $C(\boldsymbol{\lambda})\subset Q_l$. Since it is apparent that $Q_l\subset\bigcup_{\mathbf{q}\in Q_l}C(\mathbf{q})$, we have $Q_l=\bigcup_{\mathbf{q}\in Q_l}C(\mathbf{q})$. Note that, for a fixed $\mathbf{q}\in Q_l$, there are $a(\mathbf{q})-1$ more elements of Q_l that generate the same collection $C(\mathbf{q})$. Thus, by taking one element from each distinct collection, we can construct a subset Q_l' of Q_l satisfying i) $\bigcup_{\mathbf{q}\in Q_l'}C(\mathbf{q})=Q_l$ and ii) $C(\mathbf{s})\cap C(\mathbf{q})=\emptyset$ for any $\mathbf{s},\,\mathbf{q}\in Q_l'$, $\mathbf{s}\neq\mathbf{q}$.

Let μ_l be the measure of Q_l. Then, due to the independent and identically distributed (i.i.d.) uniform distribution of each element of $\boldsymbol{\lambda}$, we can see that the pdf of $\boldsymbol{\lambda}$, conditioned on $\boldsymbol{\lambda}\in Q_l$, is μ_l^{-1}. Thus, we have

$$\begin{aligned}
E\{l_r|\boldsymbol{\lambda}\in Q_l\}&=\frac{1}{\mu_l}\int_{\boldsymbol{\lambda}\in Q_l}l_r\,d\boldsymbol{\lambda}\\
&=\frac{1}{\mu_l}\int_{\boldsymbol{\lambda}\in Q_l'}\left(\sum_{\tilde{\boldsymbol{\lambda}}\in C(\boldsymbol{\lambda})}\sum_{j=1}^{J-1}l_r(\tilde\lambda_j)\right)d\boldsymbol{\lambda}.
\end{aligned}\tag{42}$$

On the other hand, we have

$$\begin{aligned}
&\sum_{\tilde{\boldsymbol{\lambda}}\in C(\boldsymbol{\lambda})}\sum_{j=1}^{J-1}l_r(\tilde\lambda_j)\\
&\quad=\sum_{j=1}^{J-1}\sum_{\tilde{\boldsymbol{\lambda}}\in C(\boldsymbol{\lambda})}l_r(\tilde\lambda_j)=\frac{a(\boldsymbol{\lambda})}{2}\sum_{j=1}^{J-1}(l_r(\lambda_j)+l_r(rT_{\mathrm{ps}}-\lambda_j))\\
&\quad=\frac{a(\boldsymbol{\lambda})}{2}\sum_{j=1}^{J-1}l_{dr}(\lambda_j)=\frac{a(\boldsymbol{\lambda})l}{2}
\end{aligned}\tag{43}$$

where the second equality follows from the fact that $a(\boldsymbol{\lambda})/2$ elements of $C(\boldsymbol{\lambda})$ take λ_j while the other $a(\boldsymbol{\lambda})/2$ elements take $rT_{\mathrm{ps}}-\lambda_j$, as their jth element.

From the definition of Q_l and Q_l', it is easily seen that $(1/\mu_l)\int_{\boldsymbol{\lambda}\in Q_l'}a(\boldsymbol{\lambda})\,d\boldsymbol{\lambda}=1$. Therefore, we get

$$\begin{aligned}
E\{l_r|l_d+l_r=l\}&=E\{l_r|\boldsymbol{\lambda}\in Q_l\}\\
&=\frac{l}{2\mu_l}\int_{\boldsymbol{\lambda}\in Q_l'}a(\boldsymbol{\lambda})\,d\boldsymbol{\lambda}=\frac{l}{2}.
\end{aligned}$$

REFERENCES

[1] V. W. S. Chan, K. L. Hall, E. Modiano, and K. A. Rauschenbach, "Architectures and technologies for high-speed optical data networks," *J. Lightwave Technol.*, vol. 16, pp. 2146–2168, Dec. 1998.

[2] P. M. Crespo, M. L. Honig, and J. A. Salehi, "Spread-time code-division multiple access," *IEEE Trans. Commun.*, vol. 43, pp. 2139–2148, June 1995.

[3] A. M. Weiner, J. P. Heritage, and J. A. Salehi, "Encoding and decoding of femtosecond pulses," *Opt. Lett.*, vol. 13, pp. 300–302, Apr. 1988.

[4] J. A. Salehi, A. M. Weiner, and J. P. Heritage, "Coherent ultrashort light pulse code-division multiple-access communication systems," *J. Lightwave Technol.*, vol. 8, pp. 478–491, Mar. 1990.

[5] H. P. Sardesai and A. M. Weiner, "Nonlinear fiber-optic receiver for ultrashort pulse code-division multiple-access communications," *Electron. Lett.*, vol. 33, pp. 610–611, Mar. 1997.

[6] G. M. Lee and G. W. Schroeder, "Optical PPM with multiple positions per pulsewidth," *IEEE Trans. Commun.*, vol. COM–25, pp. 360–364, Mar. 1977.

[7] C. N. Georghiades, "Modulation and coding for throughput-efficient optical systems," *IEEE Trans. Inform. Theory*, vol. 40, pp. 1313–1326, Sept. 1994.

[8] D. A. Fares, "Heterodyne detection of multipulse signaling in optical communication channels," *Microwave Opt. Technol. Lett.*, vol. 9, pp. 201–204, July 1995.

[9] H. M. H. Shalaby, "Maximum achievable throughputs for uncoded OPPM and MPPM in optical direct-detection channels," *J. Lightwave Technol.*, vol. 13, pp. 2121–2128, Nov. 1995.

[10] D. Shiu and J. M. Kahn, "Differential pulse-position modulation for power-efficient optical communication," *IEEE Trans. Commun.*, vol. 47, pp. 1201–1210, Aug. 1999.

[11] H. M. H. Shalaby, "Performance analysis of optical synchronous CDMA communication systems with PPM signaling," *IEEE Trans. Commun.*, vol. 43, pp. 624–634, Feb.-Apr. 1995.

[12] M. R. Dale and R. M. Gagliardi, "Channel coding for asynchronous fiber-optic CDMA communications," *IEEE Trans. Commun.*, vol. 43, pp. 2485–2492, Sept. 1995.

[13] H. M. H. Shalaby, "A performance analysis of optical overlapping PPM-CDMA communication systems," *J. Lightwave Technol.*, pp. 426–433, Mar. 1999.

[14] E. D. J. Smith, R. J. Blaikie, and D. P. Taylor, "Performance enhancement of spectral-amplitude-coding optical CDMA using pulse-position modulation," *IEEE Trans. Commun.*, vol. 46, pp. 1176–1185, Sept. 1998.

[15] K. Kamakura, T. Ohtsuki, and I. Sasase, "Optical spread time CDMA communication systems with PPM signaling," *IEICE Trans. Commun.*, vol. E82-B, pp. 1038–1047, July 1999.

[16] P. C. Sun, Y. T. Mazurenko, and Y. Fainman, "Femtoscale pulse imaging: Ultrafast optical oscilloscope," *J. Opt. Soc. Amer. A, Opt. Image Sci.*, vol. 14, pp. 1159–1170, May 1997.

[17] J.-C. Diels and W. Rudolph, *Ultrashort Laser Pulse Phenomena: Fundamentals, Techniques, and Applications on a Femtosecond Time Scale*. San Diego, CA: Academic, 1996.

[18] A. M. Weiner, D. E. Leaird, J. S. Patel, and J. R. Wullert, "Programmable femtosecond pulse shaping by use of a multielement liquid–crystal phase modulator," *Opt. Lett.*, vol. 15, pp. 326–328, Mar. 1990.

[19] F. M. Ozluturk, S. Tantaratana, and A. W. Lam, "Performance of DS/SSMA communications with MPSK signaling and complex signature sequences," *IEEE Trans. Commun.*, vol. 43, pp. 1127–1133, Feb.-Apr. 1995.

[20] J. G. Proakis, *Digital Communication*, 3rd ed. New York: McGraw-Hill, 1995.

[21] K. S. Kim, I. Song, S. C. Bang, and T.-J. Kim, "Performance analysis of forward link beamforming techniques for DS/CDMA systems using base station antenna arrays," *IEEE Trans. Signal Processing*, vol. 48, pp. 862–865, Mar. 2000.

[22] J. L. Doob, *Stochastic Processes*. New York: Wiley, 1953.

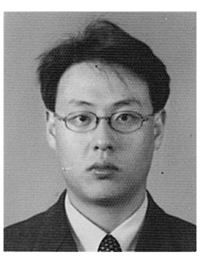

Kwang Soon Kim (S'94–M'99) was born in Seoul, Korea, on September 20, 1972. He received the B.S. (*summa cum laude*), M.S.E., and Ph.D. degrees in electrical engineering from the Korea Advanced Institute of Science and Technology (KAIST), Daejeon, Korea, in 1994, 1996, and 1999, respectively.

He was a Teaching and Research Assistant at the Department of Electrical Engineering, KAIST, from March 1994 to February 1999. From March 1999 to March 2000, he was with the Department of Electrical and Computer Engineering, University of California at San Diego, La Jolla, as a Postdoctoral Researcher. In April 2000, he joined the Mobile Telecommunication Research Laboratory, Electronics and Telecommunication Research Institute, Daejeon, Korea, where he is currently a Senior Member of Research Staff. His research interests include detection and estimation theory, channel coding and iterative decoding, array signal processing, wireless/optical CDMA systems, wireless CDMA MODEM design and development, and wireless OFDM systems.

Dr. Kim received the Postdoctoral Fellowship from the Korea Science and Engineering Foundation (KOSEF) in 1999. He also received the Silver Prize at the Humantech Paper Contest in 1998, the Silver Prize at the LG Information and Communications Paper Contest in 1998, and the Best Researcher Award from the Electronics and Telecommunication Research Institute (ETRI) in 2002.

Dan M. Marom (S'98–M'01) was born in Detroit, MI, in 1967. He received the B.Sc. and M.Sc. degrees from Tel-Aviv University, Tel-Aviv, Israel, in 1989 and 1995, respectively, and the Ph.D. degree from the University of California, San Diego (UCSD), in 2000. His doctoral dissertation dealt with femtosecond-rate optical signal processing with applications in ultrafast communications.

From 1996 through 2000, he was a Fannie and John Hertz Foundation Graduate Fellow at UCSD. In 2000, he joined Bell Laboratories, Holmdel, NJ, to pursue his interests in optical communications.

Dr. Marom received the IEEE Lasers and Electro-Optics Society Best Student Paper Award in 1999.

Laurence B. Milstein (S'66–M'68–SM'77–F'85) received the B.E.E. degree from the City College of New York, New York, NY, in 1964, and the M.S. and Ph.D. degrees in electrical engineering from the Polytechnic Institute of Brooklyn, Brooklyn, NY, in 1966 and 1968, respectively.

From 1968 to 1974, he was with the Space and Communications Group of Hughes Aircraft Company, and from 1974 to 1976, he was a member of the Department of Electrical and Systems Engineering, Rensselaer Polytechnic Institute, Troy, NY. Since 1976, he has been with the Department of Electrical and Computer Engineering, University of California at San Diego, La Jolla, where he is a Professor and former Department Chairman, working in the area of digital communication theory with special emphasis on spread-spectrum communication systems. He has also been a consultant to both government and industry in the areas of radar and communications.

Dr. Milstein was an Associate Editor for Communication Theory for the IEEE TRANSACTIONS ON COMMUNICATIONS, an Associate Editor for Book Reviews for the IEEE TRANSACTIONS ON INFORMATION THEORY, an Associate Technical Editor for the *IEEE Communications Magazine*, and the Editor-in-Chief of the IEEE JOURNAL ON SELECTED AREAS IN COMMUNICATIONS. He was the Vice President for Technical Affairs in 1990 and 1991 of the IEEE Communications Society, and has been a member of the Board of Governors of both the IEEE Communications Society and the IEEE Information Theory Society. He is a former member of the IEEE Fellows Selection Committee, and a former Chair of ComSoc's Strategic Planning Committee. He is a recipient of the 1998 Military Communications Conference Long Term Technical Achievement Award, an Academic Senate 1999 UCSD Distinguished Teaching Award, an IEEE Third Millenium Medal in 2000, the 2000 IEEE Communication Society Armstrong Technical Achievement Award, and the 2002 MILCOM Fred Ellersich Award.

Yeshaiahu Fainman (M'93–SM'01) received the Ph.D. degree from Technion-Israel Institute of Technology, Haifa, Israel, in 1983.

He is a Professor of Electrical and Computer Engineering at the University of California at San Diego, La Jolla. His current research interests are in nonlinear space–time processes using femtosecond laser pulses for optical communications, near-field phenomena in optical nanostructures and nanophotonic devices, quantum cryptography and communication, 3-D quantitative imaging, programmable, multifunctional diffractive, and nonlinear optics. He contributed over 100 manuscripts in referred journals and over 170 conference presentations and conference proceedings. Between 1993–2001, he served as a Topical Editor of the *Journal of the Optical Society of America* on Optical Signal Processing and Imaging Science.

Dr. Fainman is a Fellow of the Optical Society of America and a recipient of the Miriam and Aharon Gutvirt Prize. He served on several conferences' program committees, and organized symposia and workshops.